ethanol to give stock solutions. Actinomycin D and cycloheximide were purchased from Wakojunyaku KK, Osaka, Japan.

2.2. Cell culture

The pituitary cell line GH3 was obtained from the Health Science Research Resources Bank (Osaka, Japan) and maintained in DME/F12 mixed medium (Sigma Chemical Co.) containing penicillin and streptomycin with 10% horse serum (HS, Gibco/Invitrogen Corp., Carlsbad, CA, USA) and 2.5% fetal bovine serum (FBS, Gibco/Invitrogen). Before estrogen treatment, cells were maintained for a week in phenol red-free medium (Sigma Chemicals) containing the same antibiotics along with dextran-charcoal-treated serum. For cell growth assays, GH3 cells were seeded in 24-well plates at 1×10^4 cells/well, and hormones were added the next day. Growth was measured after five days by means of a modified MTT assay with WST-1 (Dojindo Chemicals, Kumamoto, Japan). For microarray analysis, 3×10^6 GH3 cells were seeded in 90 mm dishes and treated with E2 at 10^{-9} M and/or ICI at 10^{-7} M and harvested after 24 h treatment. Cells were harvested after addition of Isogen (Wakojunyaku). For mRNA quantification, cells were treated with E2 at 10^{-12} to 10^{-9} M and/or ICI182780 at 10^{-7} M. After the indicated period of time, cells were harvested with cell lysis buffer supplied with an SV-total RNA isolation kit (Promega Co., Madison, WI, USA).

2.3. Animals

Animal experiments were conducted under the guidelines of the 'A Guide for the Care and Use of Laboratory Animals of Hiroshima University'. Female F344 rats were purchased at four weeks of age from Charles River Japan Co.. (Kanagawa, Japan). They were maintained with free access to basal diet and tap water. All animals except the intact control underwent surgical ovariectomy upon receipt and implanted with pellets containing 10 mg of E2 subcutaneously as described previously [16]. Animals were sacrificed under ether anesthesia after 3, 8, 24 and 48 h in the short-term experiment. Treatment was extended between 7 and 30 days for the long-term experiment. The pituitary gland and the uterus of each rat were weighed and immediately frozen in liquid nitrogen and stored at −80 °C.

2.4. The GeneChip analysis

Total RNAs were extracted with Isogen, a premixed RNA isolation reagent, based on the acid guanidium thiocyanate–phenol–chloroform extraction method. The supplied protocol was followed.

First-strand cDNA was synthesized by incubating 5 μg of total RNAs with 200 U SuperScript II reverse transcriptase (Invitrogen, Carlsbad, CA), 100 pmol T7-(dT)24 primer [5′-GGCCAGTGAATTGTAATACGACTCACTATAGGGAGGCGG-(dT)24-3′], 1 × first-strand buffer (50 mM Tris–HCl pH 8.3, 75 mM KCl, 3 mM MgCl2, 10 mM DTT) and 0.5 mM dNTPs at 42 °C for 1 h. Second-strand synthesis was performed by incubating the first-strand cDNAs with 10 U *E. coli* ligase (Invitrogen), 40 U DNA polymerase I (Invitrogen), 2 U RNase H (Invitrogen), 1× reaction buffer (18.8 mM Tris–HCl pH 8.3, 90.6 mM KCl, 4.6 mM $MgCl_2$, 3.8 mM DTT, 0.15 mM NAD, 10 mM $(NH_4)_2SO_4$) and 0.2 mM dNTPs at 16 °C for 2 h. Ten units of T4 DNA polymerase (Invitrogen) were then added, and the reaction was allowed to continue for another 5 min at 16 °C. After phenol–chloroform extraction and ethanol precipitation, the double-stranded cDNA was resuspended in 12 μl DEPC-treated dH_2O. Labeling of the dsDNA was achieved by in vitro transcription using a BioArray HighYield RNA transcript labeling kit (Enzo Diagnostics, Farmingdale, NY). Briefly, the dsDNA was mixed with 1× HY reaction buffer, 1× biotin labeled ribonucleotides (NTPs with Bio-UTP and Bio-CTP), 1× DTT, 1× RNase inhibitor mix and 1× T7 RNA polymerase. The mixture was incubated at 37 °C for 4 h. The labeled cRNA was then purified using a RNeasy mini kit (Qiagen, Valencia, CA) according to the manufacturer's instructions. The purified cRNA was fragmented in 1 × fragmentation buffer (40 mM acetate, 100 mM KOAc, 30 mM MgOAc) at 94 °C for 35 min. For hybridization with the GeneChip Rat Genome U34A (Affymetrix), 15 μg fragmented cRNA probe was incubated with 50 pM control oligonucleotide B2, 1× eukaryotic hybridization control (1.5 pM BioB, 5 pM BioC, 25 pM BioD and 100 pM Cre), 0.1 mg/ml herring sperm DNA, 0.5 mg/ml acetylated BSA and 1× manufacturer-recommended hybridization buffer in a 45 °C rotisserie oven for 16 h. Washing and staining were performed with a GeneChip Fluidic Station (Affymetrix) using the appropriate antibody amplification washing and staining protocol. The phycoerythrin-stained arrays were scanned as digital image files and scanned data were analyzed with GeneChip software (Affymetrix) [17].

2.5. Quantification of mRNAs by real-time RT-PCR

RNA preparation was carried out with an SV-total RNA isolation kit. One microgram of total RNA was reverse-transcribed with 200 U of MMLV-RT (Invitrogen) and 2.5 pmol of oligo-dT primer (Invitrogen) in 25 μl buffer containing 1 mM dNTP, 100 mM Tris–HCl (pH 8.3), 150 mM KCl, 6 mM $MgCl_2$, 60 mM dithiothreitol and 5 U/μl RNasin with incubation at 37 °C for 60 min.

The real-time PCR method with a QuantiTect Sybr Green PCR kit (Qiagen) and an ABI Prism 7700 (The Perkin–Elmer Co) was employed for quantitative measurement for following the supplied protocol [18]. Specific primer sets with a T_m of about 59 °C were designed for each mRNA selected from the microarray analysis (Table 1). The PCR conditions were a 15 min of initial activation step followed by 45 cycles of 15 s at 94 °C, 30 s at 50 °C and 60 s at

Table 1
Nucleotide sequences of primers for quantitative real-time PCR

Gene	GenBank accession#	Forward	Reverse
#1	K00994	AACCAGCTGTCCAAGGAGGA	CTTCTCCATCATCGTTCTTATCCA
#2	AI175539	TTTCTTCAGGCCCACCATCT	TTGCAGGATGTCGATGACAGA
#3	AI014135	GAACCAATTCTCCTAGCACAAGTG	CACGCCTGTGTTGGGCTAA
#4	AI178971	GGTGTGAAATCCCCAGGGT	CCCTGTCCACTCTGAGCGAC
#5	S81478	GATCAACGTCTCGGCCAATT	GCACAAACACCCTTCCTCCA
#6	D26393	GATTTCTAGGCGGTTCCGGA	ACTCGGAGCACACGGAAGTT
#7	AI230712	TGGCAGAAAAATCAATCCAGC	AAAGCCAGCCCCAAATCAC
#8	AF081366	CATCTGGACAACTGTGCTGGA	GGCACCACACATGAAGGAATT
#9	Y00396	CCGAGCTACTTGGAGGAGACA	AGGCCAGCTTCTCGGAGAC
#10	U02553	GATCAACGTCTCGGCCAATT	GCACAAACACCCTTCCTCCA
#14	U24175	CAGTGGATCGAGAGCCAGC	TGCCCCAGCTTGATCTTCAG
#15	D13623	ACCAAGACCGGTAGCAAGGG	GAAATCCGACGGAAGAGTGC
#21	AA892522	CCTTCGACTCAGCCACAAAAA	ACAGGGTCTTACCCTGCCTTC
#22	L16922	AGCCAGAGCCCACAATATGG	GCAATCATTTCTTCCGGCAC
G3PDH	AB017801	TGAAGGTCGGTGTGAACGGATTTG	TGATGGCATGGACTGTGGTCATGA

72 °C. Prior to the quantitative analysis, PCR products were prepared separately and purified by gel electrophoresis. The fragments extracted from the gel were used as standards for quantification. The DNA sequences were confirmed with a capillary DNA sequencer, ABI 310 (The Perkin–Elmer Co.). All mRNA contents were normalized with reference to G3PDH mRNA.

2.6. Statistical analysis

Multiple comparison was made by ANOVA followed by Scheffe's test. Otherwise, Student's *t*-test was applied.

3. Results

3.1. Estrogen-dependent cell proliferation of GH3

The relative cell numbers were measured at day 5 of treatment with E2 at concentrations from 10^{-13} to 10^{-9} M (Fig. 1). Significant stimulation of cell proliferation was observed at 10^{-12} M and the response appeared to reach a maximum at 10^{-11} M. The sizes of individual cells treated with E2 appeared to be larger than without hormone.

3.2. Estrogen-responsive genes identified by cDNA microarray

Differentially expressed genes based on the ratio of the measured hybridization intensities on GeneChip Rat Genome U34A between control and E2-treated cells are listed in Table 1. A minimal change of two-fold was applied to select up- and down-regulated genes. Two independent experiments were carried out and the genes showing reliable hybridization for both experiments were counted. The genes are listed according to average values of E2 induction. The results of ICI182780 treatment alone or with E2 are also given in Table 2. The genes regulated by E2 but not showing inhibition by ICI182780, which only accounted for four in total, are not included in the table. Interestingly, only 26 genes were categorized as up-regulated and seven as the down-regulated, out of approximately 8000 genes on the chip.

3.3. Confirmation of mRNA changes

From Table 2, the top ten genes and four others (#14, #15, #21 and #22) were selected and subjected to quantification of mRNA levels to confirm the results of cDNA microarray analysis. cDNAs from GH3 cells treated with E2 at 10^{-12} to 10^{-9} M and/or ICI at 10^{-7} M are examined and

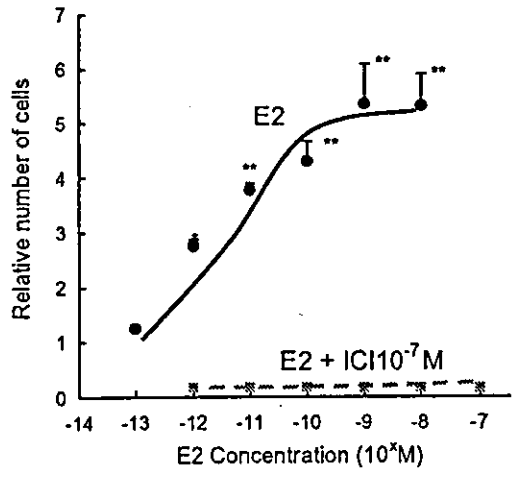

Fig. 1. Effects of 17β-estradiol (E2) and ICI182780 (ICI) on GH3 cell proliferation. Cells were seeded in 24-well plates at 1×10^4 cells per well. After five days treatment with E2 at 10^{-13} to 10^{-9} M alone or with ICI at 10^{-7} M, cell proliferation was measured by a modified MTT assay. Each point represents a mean ± S.E.M. ($n = 4$). *,** Indicates significant differences from the control value at 0.05 and 0.01, respectively.

Table 2
Genes up- and down-regulated by estrogen two or more fold in the microarray study

Genbank accession#		Gene name/blast match	Fold change in expression			
			E2(Exp1)	E2(Exp2)	E2+ICI	ICI
Genes up-regulated						
#1	K00994	Calbindin-D9k*	8.12	6.20	0.70	0.33
#2	AI175539	Parvalbumin*	7.58	4.54	0.81	0.28
#3	AI014135	Ribosomal RNA*	6.23	4.93	1.17	0.94
#4	M17083	Alpha globin*	5.23	4.99	0.39	0.59
#5	S81478	3CH134/CL1 ATPase	4.77	4.12	0.97	1.11
#6	D26393	Type II hexokinase	2.75	3.15	0.14	0.49
#7	AI230712	PACE4*	2.98	2.73	0.44	0.15
#8	AF081366	K + channel ROMK2.1 isoform	3.21	2.44	0.88	0.20
#9	Y00396	c-*myc* protein	2.99	2.59	0.76	0.35
#10	U02553	Protein tyrosine phosphatase	3.32	2.23	0.67	0.44
#11	AF036548	RGC-32	3.47	2.05	1.12	0.37
#12	U53505	Type II iodothyronine deiodinase	2.26	2.87	0.77	0.34
#13	Y09507	Hypoxia-inducible factor 1	2.60	2.38	1.13	0.69
#14	U24175	Regulator of transcription 5a1	2.77	2.01	0.61	0.46
#15	D13623	p34 protein	2.43	2.32	1.05	1.02
#16	M58040	Transferrin receptor	2.37	2.38	0.73	0.30
#17	AA819776	EST (similar to HSP86)	1.93	2.76	1.82	1.97
#18	AA875126	EST (unknown)	2.33	2.27	0.58	0.70
#19	M14656	Osteopontin	1.89	2.69	1.37	1.22
#20	X67788	Ezrin, p81	2.28	2.23	0.47	0.50
#21	AA892522	EST (unknown)	2.19	2.23	0.60	0.82
#22	L16922	Progesterone receptor	2.30	2.04	0.89	0.67
#23	U57097	APEG-1 protein	2.36	1.97	1.43	1.51
#24	M24852	Neuron-specific protein	1.87	2.45	1.73	1.57
#25	AA817846	EST (similar to D-β-hydroxy butyrate dehydrogenase)	1.86	2.37	0.97	0.96
#26	AI169417	Phosphoglycerate mutase type B subunit mRNA*	1.98	2.23	0.97	0.92
Genes down-regulated						
	U67080	Zinc finger protein r-MyT3	0.49	0.47	1.38	1.06
	AA799964	EST (unknown)	0.49	0.41	0.51	0.71
	AI639263	EST (unknown)	0.46	0.41	0.68	0.32
	M27925	Synapsin 2a	0.47	0.35	1.31	1.31
	E03229	JP 1991272688-A/2	0.47	0.30	1.31	0.95
	AI237654	Vdup1*	0.40	0.35	0.81	0.84
	AA893280	EST (similar to adipose differenti-ation-related protein)	0.47	0.21	0.91	0.98

Gene are listed in order of average E2 fold change in Experiments 1 and 2. **Four E2 up-regulated genes were not inhibited by ICI, which are not included in this table (The GenBank accession numbers of these are AI138070, AA866485, D84480 and X74293).
* Indicates genes originally listed as ESTs but found to have perfect match by BLAST.

the results were summarized in Fig. 2. Although the fold increases of E2 induced gene expression were slightly lower than in the microarray analysis, up-regulation and inhibition by ICI182780 were confirmed except with three genes, #3, #6 and #15, which showed no responses. Time dependence of gene expression induced by E2 was also examined and the results are summarized in Fig. 3. As expected, some of the genes were expressed early after E2 administration and others increased gradually. Since the microarray analysis was carried out at only one time point, 24 h after E2 treatment, early responding and quickly muting genes would not be expected to be identified.

To determine E2 in inducing the transcription of genes #1 and #2, GH3 cells were treated with E2 in the presence of 0.5 μg/ml of actinomycin D (a transcription inhibitor) and 10 μg/ml cycloheximide (a translation inhibitor) for 3 and 24 h (Table 3). Increase in mRNA levels by E2 was blocked

Table 3
Effects of cycloheximide and actinomycin D on E2-induced mRNA change of calbindin D9k and parvalbumin in GH3 cells

	3 h	24 h
Gene#1: calbindin D9k		
Control	5.45 ± 0.70**	4.02 ± 0.33**
CHX	4.03 ± 0.11**	3.74 ± 0.27**
ActD	1.01 ± 0.21	1.13 ± 0.23
Gene#2: parvalbumin		
Control	1.81 ± 0.41	4.52 ± 0.94*
CHX	2.51 ± 0.19**	8.34 ± 0.37**
ActD	0.93 ± 0.09	1.58 ± 0.31

Cell were treated with E2 at 10^{-9} M for 3 and 24 h with or without cycloheximide (CHX) at 10 μg/ml or actinomycin D (ActD) at 0.5 μg/ml. The inductions by E2 were calculated for each treatment (mean ± S.E.M., $n = 4$).
* Indicates significant induction at 0.05 and 0.01, respectively.
** Indicates significant induction at 0.05 and 0.01, respectively.

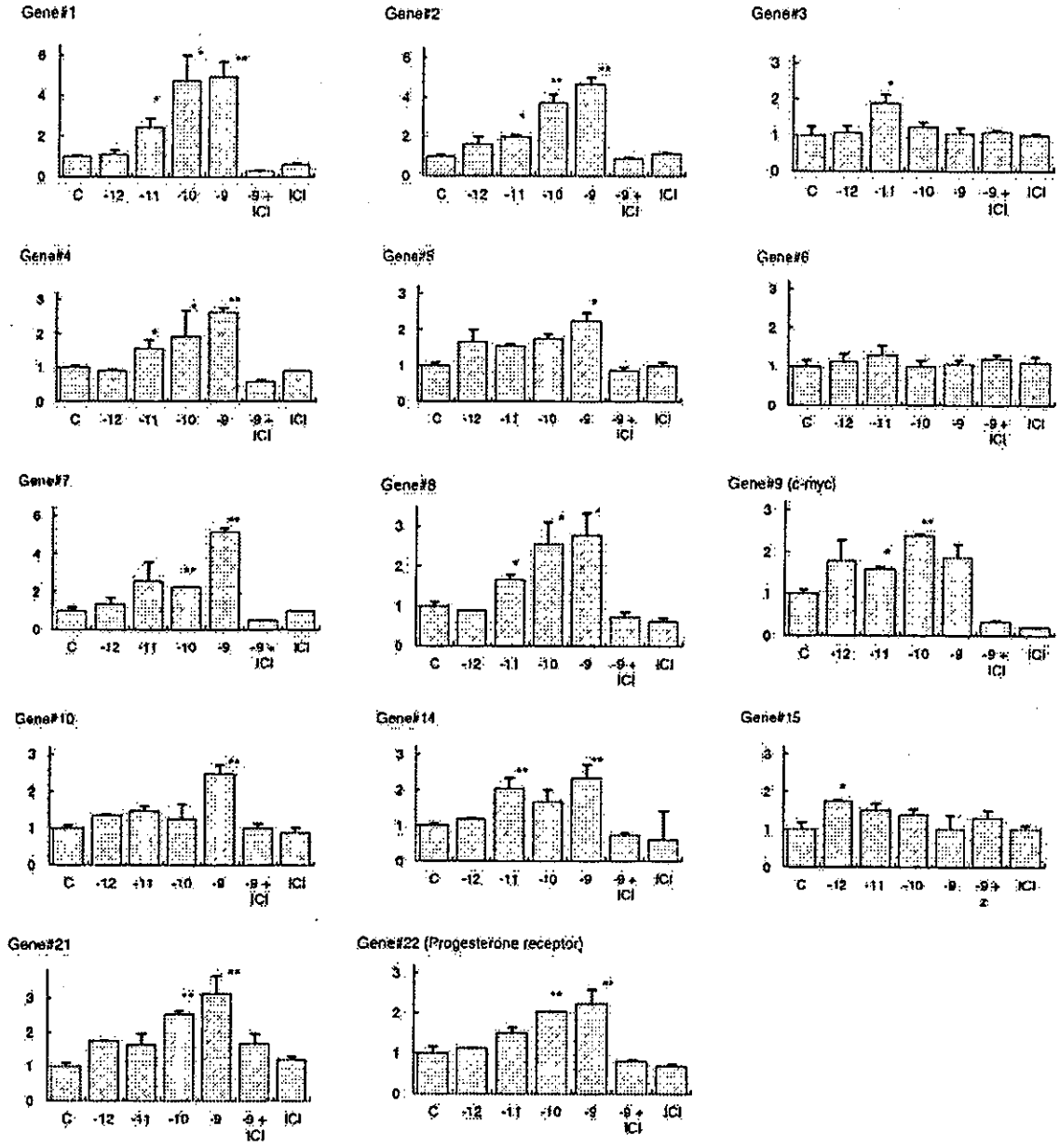

Fig. 2. Dose-dependent changes in gene expression levels measured by quantitative real-time RT-PCR. Cells were treated with different concentrations of E2 at 10^{-12} to 10^{-9} M and/or a single dose of ICI 182780 (ICI) at 10^{-7} M for 24 h. All mRNA contents were normalized with reference to G3PDH mRNA. The fold changes were calculated based on the gene expression in the cells treated with vehicle. Each point is an average of two independent experiments.

by actinomycin D but not by cycloheximide, which indicates that E2 regulates these genes at the transcriptional level.

3.4. Expression of genes in the pituitary gland

Expression of estrogen regulated genes in GH3 cells was further investigated in the anterior pituitary gland. First, mRNA expression of eleven-responsive genes was examined in short-term (24 h) and long-term (30 days) E2-treated ovariectomized F344 rats. Findings for estrogen-dependent increase for each gene are summarized in Table 4 as fold change of mRNA in E2-treated animals over that in the ovariectomized controls. All the genes except #4 were up-regulated in pituitary tissue by the short-term and long-term treatment of E2. Estrogen dependence of expression of gene #1 (calbindin-D9k) and gene #2 (parvalbumin) was extremely strong, over 100-fold induction being noted. For these and gene #9 (c-*myc*), more detailed time-dependent analysis was carried out. In Fig. 4, each mRNA level was calculated based on the level in ovariectomized rats at day

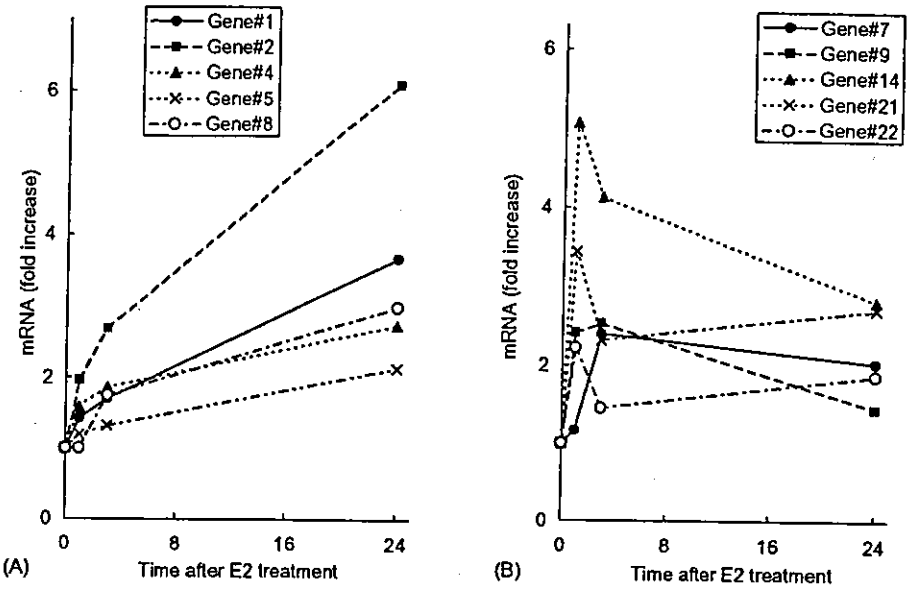

Fig. 3. Time-dependent change in gene expression levels measured by quantitative real-time RT-PCR. All mRNA contents were normalized with reference to G3PDH mRNA. Cells were treated with E2 at 10^{-9} M for 0, 1, 3 and 24 h. Each point represents a mean ± S.E.M. ($n = 4$). *,** Indicates significant differences from the control values at 0.05 and 0.01, respectively.

Table 4
Estrogen-responsive genes identified by the microarray study in the pituitary tissues in ovariectomized F344 rats

Gene	GenBank accession#	Fold change in expression	
		24 h	1 month
#1	K00994	118	95.0
#2	AI175539	28.9	70.0
#4	M17083	1.1	0.6
#5	S81478	2.3	2.0
#7	AI230712	2.9	4.7
#8	AF081366	9.9	2.0
#9	Y00396	4.5	17.7
#10	U02553	3.1	1.6
#14	U24175	2.4	4.0
#21	AA892522	2.0	5.1
#22	L16922	4.2	9.4

Ovariectomized F344 rats were treated subcutaneously with pellets containing E2 for 1 and 30 days. The gene expression was measured by quantitative real-time RT-PCR in pituitary tissue and the fold changes were calculated based on the mRNA level in ovariectomized controls at time 0 ($n = 5$).

0. All the three mRNAs, for calbindin-D9k, parvalbumin and c-*myc*, were induced significantly within 3 h of subcutaneous E2 administration, although the increase was most prominent for calbindin-D9k, with a 72-fold elevation. Higher levels were still maintained after a month of chronic E2 treatment.

4. Discussion

The GH3 cell line has been widely used to investigate the functions of somatolactotrophic cells, since regulation of its GH and prolactin production appears to be physiologically relevant with dependence on thyroid hormones, estrogen and glucocorticoid [11,12,19]. In the present study, we applied microarray analysis and identified a number of estrogen-responsive genes.

In terms of GH3 estrogen-responsiveness, there are two distinct parameters, prolactin synthesis and cell proliferation. However, reported sensitivity to estrogen has varied in the literature [4,13–15,20]. The inter-laboratory variation may be due partly to differences in strain, since GH3 has a rather old origin and has been widely used. Technical problems with charcoal treatment of serum for removing estrogenic substances may have had an impact in some cases [21]. The estrogenic activity of phenol red or related contaminants in common culture media was not recognized until Katzenellenbogen's group provided a convincing evidence [22]. Prior to the present microarray analysis, GH3 cells were examined in our culture conditions and found to be very sensitive to estrogen, exhibiting induction of cell proliferation in response to E2 at a concentration as low as 10^{-12} M. The high sensitivity on cell proliferation appears typical for pituitary cell lines, like the MtT/E-2 cell line we have established and another lactotrophic cell line, PR1 [4,23]. ERα is the major type of ER expressed in GH3 cells with a ratio to ERβ of 380:1 according to quantitative PCR (data not shown).

Recently, estrogen-responsive genes have been investigated by cDNA microarray in human breast cancers and the normal uterus [24,25]. However, the pituitary gland has not been explored for estrogen-responsive genes by this approach, to our knowledge. In the present microarray analysis, a relatively small number of genes were found to be

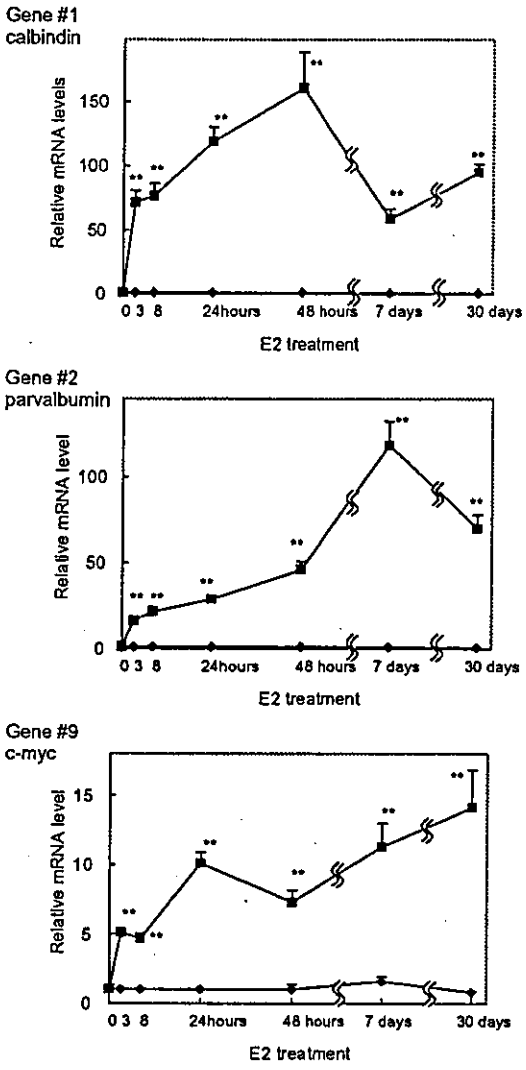

Fig. 4. Time-dependent analysis of three estrogen-responsive genes in the pituitary in vivo. Ovariectomized F344 rats were treated subcutaneously with pellets containing E2 for 3, 8, 24, and 48 h and 7 and 30 days. Gene expression was measured by quantitative real-time RT-PCR in pituitary tissue and fold changes were calculated based on the mRNA level in the ovariectomized controls at time zero. All mRNA contents were normalized with reference to G3PDH mRNA. Each point and bar represent mean ± S.E.M. ($n = 5$), *,** Indicates significant differences from the control values at 0.05 and 0.01, respectively.

regulated by estrogen with confirmation in most cases by quantitative real-time PCR. Suppression by ICI of E2-induced gene expression was also confirmed. The degrees of change were similar with real-time PCR analysis and GeneChip data and although we selected up-regulated genes after 24 h of estrogen exposure, some genes proved to be rapidly regulated (Fig. 3(B)) including these for the progesterone receptor and c-*myc*. Estrogen-responsive induction of progesterone receptor is well documented for the primary target, the uterus, as well as in the anterior pituitary gland [26,27]. Estrogen activation of c-*myc* also has been reported in the anterior pituitary gland and breast cancer cells [28,29]. A total of seven genes could be listed as down-regulated but they were not analyzed further, since all of them displayed relatively small degrees of change to 0.34–0.48 of the control values. Other known estrogen-responsive genes in the pituitary gland, such as prolactin and TGFα were not on the array used in the present study.

Interestingly, the in vivo expression of two genes, calbindin-D9k and parvalbumin, was found to be highly induced by E2 both in the short and longer term, which may suggest that hypothalamus or other indirect endocrine pathways would be involved in regulating genes in addition to the direct transcriptional activation. Calbindin-D9k is a vitamin D-dependent intestinal calcium-binding protein that is detectable in the duodenum, uterus and placenta [30–32]. Another vitamin D-dependent calcium-binding protein, calbindin-D28k, expressed in kidney and brain has no homology with calbindin-D9k either at the nucleotide or at the transcript levels [33]. The calbindin-D9k gene has been reported to contain a 15-base-pair imperfect palindrome with high homology to the estrogen- and glucocorticoid-responsive elements (ERE and GRE) [34]. Although there is no evidence that this protein is regulated by estrogen in the intestine through this motif, it is possible that the imperfect ERE is functional for the hormone-dependent transcription in the pituitary gland. Parvalbumin is another calcium-binding protein that belongs to the EF-hand calcium-binding protein like calbindin-D9k [35]. It is abundant in fast contracting/relaxing muscle fibers, where it plays a role as a calcium buffer and is also found in neurons as well as in endocrine glands including pituitary, thyroid, adrenals, testes and ovaries [36]. It has been postulated that parvalbumin can prevent cell death due to calcium overload in neurons. Although its expression is developmentally regulated in muscle, brain and other tissues, no evidence indicating hormonal regulation has been reported [37,38]. The 5′ flanking region of the gene seems to function as the promoter but it does not contain any motifs for estrogen-dependent transcription [39,40].

Since RNA was extracted from whole anterior pituitary tissue in the present study, it is not clear which types of cell actually contributed to the increase in mRNA levels. Chronic treatment of rats with E2 is known to result in the development of lactotrophic tumors [5]. The F344 strain is the most sensitive to E2 and somatolactotrophs of the pituitary become hyperplastic after exposure for a week and steadily proliferate thereafter. In the present study, major response of GH3 cells was cell proliferation so that some of the identified genes might be expected to be mitosis-related and involved in estrogen-induced pituitary hyperplasia/tumorigenesis. Although up-regulation of the calbindin-D9k and parvalbumin gene are evident on long-term treatment of E2, there was no obvious correlation with the time period for pituitary hyperplasia in contrast to the c-*myc* expression which steadily increase.

In conclusion, the present microarray analysis allowed identification of a number of estrogen-responsive genes in GH3 cells whose regulation appears biologically relevant in the pituitary gland in vivo. The actual significance of two calcium-binding proteins discovered to be prominently induced by E2 remains to be explored in the future.

Acknowledgements

We thank Mr. Y. Mizuno for his expert technical assistance and Dr. M.A. Moore for reading the manuscript and suggesting English clarification. This work was supported, in part, by Grant-in-Aid (H13-Seikatsu) from the Ministry of Health, Labor and Welfare, Japan and a Grant-in-Aid (#14042241) from the Ministry of Education, Culture, Sports, Science and Technology, Japan.

References

[1] W.L. Miller, M.M. Knight, J. Gorski, Estrogen action in vitro: regulation of thyroid stimulating and other pituitary hormones in cell cultures, Endocrinology 101 (1977) 1455–1460.
[2] K.M. Scully, A.S. Gleiberman, J. Lindzey, D.B. Lubahn, K.S. Korach, M.G. Rosenfeld, Role of estrogen receptor-alpha in the anterior pituitary gland, Mol. Endocrinol. 11 (1997) 674–681.
[3] D.L. Allen, N.A. Mitchner, T.E. Uveges, K.P. Nephew, S. Khan, J.N. Ben, Cell-specific induction of c-*fos* expression in the pituitary gland by estrogen, Endocrinology 138 (1997) 2128–2135.
[4] T.Y. Chun, D. Gregg, D.K. Sarkar, J. Gorski, Differential regulation by estrogens of growth and prolactin synthesis in pituitary cells suggests that only a small pool of estrogen receptors is required for growth, Proc. Natl. Acad. Sci. USA 95 (1998) 2325–2330.
[5] M.E. Lieberman, R.A. Maurer, P. Claude, J. Wiklund, N. Wertz, J. Gorski, Regulation of pituitary growth and prolactin gene expression by estrogen, Adv. Exp. Med. Biol. 138 (1981) 151–163.
[6] C.L. Bethea, Stimulatory effect of estrogen on prolactin secretion from primate pituitary cells cultured on extracellular matrix and in serum-free medium, Endocrinology 115 (1984) 443–451.
[7] T.J. Spady, K.L. Pennington, R.D. McComb, J.D. Shull, Genetic bases of estrogen-induced pituitary growth in an intercross between the ACI and Copenhagen rat strains: dominant mendelian inheritance of the ACI phenotype, Endocrinology 140 (1999) 2828–2835.
[8] S. Holtzman, J.P. Stone, C.J. Shellabarger, Influence of diethylstilbestrol treatment on prolactin cells of female ACI and Sprague-Dawley rats, Cancer Res. 39 (1979) 779–784.
[9] R.V. Lloyd, K. Coleman, K. Fields, V. Nath, Analysis of prolactin and growth hormone production in hyperplastic and neoplastic rat pituitary tissues by the hemolytic plaque assay, Cancer Res. 47 (1987) 1087–1092.
[10] J. Tashjian-AH, Y. Yasumura, L. Levine, G.H. Sato, M.L. Parker, Establishment of clonal strains of rat pituitary tumor cells that secrete growth hormone, Endocrinology 82 (1968) 342–352.
[11] J.M. Sorrentino, W.L. Kirkland, D.A. Sirbasku, Control of cell growth. II. Requirement of thyroid hormones for the in vivo estrogen-dependent growth of rat pituitary tumor cells, J. Natl. Cancer Inst. 56 (1976) 1155–1158.
[12] E. Haug, K.M. Gautvik, Effects of sex steroids on prolactin secreting rat pituitary cells in culture, Endocrinology 99 (1976) 1482–1489.
[13] D.R. Kiino, P.S. Dannies, Insulin and 17 beta-estradiol increase the intracellular prolactin content of GH4C1 cells, Endocrinology 109 (1981) 1264–1269.
[14] P.R. Rhode, J. Gorski, Growth and cell cycle regulation of mRNA levels in GH3 cells, Mol. Cell Endocrinol. 82 (1991) 11–22.
[15] J.G. Scammell, T.G. Burrage, P.S. Dannies, Hormonal induction of secretory granules in a pituitary tumor cell line, Endocrinology 119 (1986) 1543–1548.
[16] N. Fujimoto, H. Watanabe, A. Ito, K. Inoue, Estrogen receptor levels and tumor growth in a series of pituitary clonal cell lines in rats, Jpn. J. Cancer Res. 82 (1991) 1436–1441.
[17] D.J. Lockhart, H. Dong, M.C. Byrne, M.T. Follettie, M.V. Gallo, M.S. Chee, M. Mittmann, C. Wang, M. Kobayashi, H. Horton, E.L. Brown, Expression monitoring by hybridization to high-density oligonucleotide arrays, Nat. Biotechnol. 14 (1996) 1675–1680.
[18] T.H. Woo, B.K. Patel, M. Cinco, L.D. Smythe, M.L. Symonds, M.A. Norris, M.F. Dohnt, Real-time homogeneous assay of rapid cycle polymerase chain reaction product for identification of *Leptonema illini*, Anal. Biochem. 259 (1998) 112–117.
[19] E. Haug, O. Naess, K.M. Gautvik, Receptors for 17β-estradiol in prolactin-secreting rat pituitary cells, Mol. Cell Endocrinol. 12 (1978) 81–95.
[20] J.F. Amara, I.C. Van, P.S. Dannies, Regulation of prolactin production and cell growth by estradiol: difference in sensitivity to estradiol occurs at level of messenger ribonucleic acid accumulation, Endocrinology 120 (1987) 264–271.
[21] T.L. Riss, D.A. Sirbasku, Rat pituitary tumor cells in serum-free culture. II. Serum factor and thyroid hormone requirements for estrogen-responsive growth, In Vitro Cell Dev. Biol. 25 (1989) 136–142.
[22] Y. Berthois, J.A. Katzenellenbogen, B.S. Katzenellenbogen, Phenol red in tissue culture media is a weak estrogen: implications concerning the study of estrogen-responsive cells in culture, Proc. Natl. Acad. Sci. USA 83 (1986) 2496–2500.
[23] N. Fujimoto, S. Maruyama, A. Ito, Establishment of an estrogen-responsive rat pituitary cell sub-line MtT/E-2, Endocr. J. 46 (1999) 389–396.
[24] H. Watanabe, A. Suzuki, M. Kobayashi, E. Takahashi, M. Itamoto, D.B. Lubahn, H. Handa, T. Iguchi, Analysis of temporal changes in the expression of estrogen-regulated genes in the uterus, J. Mol. Endocrinol. 30 (2003) 347–358.
[25] A. Inoue, N. Yoshida, Y. Omoto, S. Oguchi, T. Yamori, R. Kiyama, S. Hayashi, Development of cDNA microarray for expression profiling of estrogen-responsive genes, J. Mol. Endocrinol. 29 (2002) 175–192.
[26] L.A. Denner, W.T. Schrader, B.W. O'Malley, N.L. Weigel, Hormonal regulation and identification of chicken progesterone receptor phosphorylation sites, J. Biol. Chem. 265 (1990) 16548–16555.
[27] E. Vegeto, M.M. Shahbaz, D.X. Wen, M.E. Goldman, B.W. O'Malley, D.P. McDonnell, Human progesterone receptor A form is a cell- and promoter-specific repressor of human progesterone receptor B function [see comments], Mol. Endocrinol. 7 (1993) 1244–1255.
[28] I. Szijan, D.L. Parma, N.I. Engel, Expression of c-*myc* and c-*fos* protooncogenes in the anterior pituitary gland of the rat. Effect of estrogen, Horm. Metab. Res. 24 (1992) 154–157.
[29] D. Dubik, R.P. Shiu, Mechanism of estrogen activation of c-*myc* oncogene expression, Oncogene 7 (1992) 1587–1594.
[30] A.C. Delorme, J.L. Danan, M.G. Acker, M.A. Ripoche, H. Mathieu, In rat uterus 17β-estradiol stimulates a calcium-binding protein similar to the duodenal vitamin D-dependent calcium-binding protein, Endocrinology 113 (1983) 1340–1347.
[31] M.E. Bruns, A. Fausto, L.V. Avioli, Placental calcium binding protein in rats. Apparent identity with vitamin D-dependent calcium binding protein from rat intestine, J. Biol. Chem. 253 (1978) 3186–3190.
[32] M. Davie, Calcium-ion-binding activity in human small-intestinal mucosal cytosol. Purification of two proteins and interrelationship of calcium-binding fractions, Biochem. J. 197 (1981) 55–65.

[33] N. Lomri, C. Perret, N. Gouhier, M. Thomasset, Cloning and analysis of calbindin-D28K cDNA and its expression in the central nervous system, Gene 80 (1989) 87–98.
[34] J. Krisinger, H. Darwish, N. Maeda, H.F. DeLuca, Structure and nucleotide sequence of the rat intestinal vitamin D-dependent calcium binding protein gene, Proc. Natl. Acad. Sci. USA 85 (1988) 8988–8992.
[35] M.W. Berchtold, A.R. Means, The Ca^{2+}-binding protein parvalbumin: molecular cloning and developmental regulation of mRNA abundance, Proc. Natl. Acad. Sci. USA 82 (1985) 1414–1418.
[36] T. Endo, K. Takazawa, T. Onaya, Parvalbumin exists in rat endocrine glands, Endocrinology 117 (1985) 527–531.
[37] M. Sano, T. Yokota, T. Endo, H. Tsukagoshi, A developmental change in the content of parvalbumin in normal and dystrophic mouse (mdx) muscle, J. Neurol. Sci. 97 (1990) 261–272.
[38] V. Pohl, G. Pattyn, M. Berchtold, Parvalbumin expression during developmental differentiation of the rat ovary, Differentiation 59 (1995) 235–242.
[39] M.W. Berchtold, Parvalbumin genes from human and rat are identical in intron/exon organization and contain highly homologous regulatory elements and coding sequences, J. Mol. Biol. 210 (1989) 417–427.
[40] M. Schleef, C. Zuhlke, H. Jockusch, F. Schoffl, The structure of the mouse parvalbumin gene, Mamm. Genome 3 (1992) 217–225.

Senescent B Lymphopoiesis Is Balanced in Suppressive Homeostasis: Decrease in Interleukin-7 and Transforming Growth Factor-β Levels in Stromal Cells of Senescence-Accelerated Mice

ISAO TSUBOI,*,† KOHJI MORIMOTO,* YOKO HIRABAYASHI,* GUANG-XUN LI,* SHIN AIZAWA,† KAZUHIRO J. MORI, JUN KANNO,* AND TOHRU INOUE§,[1]

Division of Cellular and Molecular Toxicology, National Institute of Health Sciences, Tokyo 158–8501, Japan; †Department of Anatomy and Developmental Biology, Nihon University School of Medicine, Tokyo 173–8610, Japan; Department of Molecular and Cellular Biology, Faculty of Science, Niigata University, Niigata 950–2181, Japan; and §Center for Biological Safety and Research, National Institute of Health Sciences, Tokyo 158–8501, Japan

The suppression of the B cell population during senescence has been considered to be due to the suppression of interleukin-7 (IL-7) production and responsiveness to IL-7; however, the upregulation of transforming growth factor-β (TGF-β) was found to contribute to B cell suppression.To investigate the mechanism of this suppression based on the interrelationship between IL-7 and TGF-β during senescence, senescence-accelerated mice (SAMs), the mouse model of aging, were used in this study to elucidate the mechanisms of B lymphopoietic suppression during aging. Similar to regular senescent mice, SAMs showed a decrease in the number of IL-7–responding B cell progenitors (i.e., colony-forming unit pre-B [CFU-pre-B] cells in the femoral bone marrow [BM]). A co-culture system of B lymphocytes and stromal cells that the authors established showed a significantly lower number of CFU-pre-B cells harvested when BM cells were co-cultured with senescent stromal cells than when they were co-cultured with young stromal cells. Interestingly, cells harvested from a senescent stroma and those from the control culture without stromal cells were higher in number than those harvested from a young stroma, thereby implying that an altered senescent stromal cell is unable to maintain self-renewal of the stem cell compartment. Because TGF-β is supposed to suppress the proliferative capacity of pro-B/pre-B cells, we added a neutralizing anti-TGF-β antibody to the co-culture system with a pro-B/pre-B cell-rich population to determine whether such suppression may be rescued. However, unexpectedly, any rescue was not observed and the number of CFU-pre-B cells remained unchanged when BM cells were co-cultured with senescent stromal cells compared with the co-culture with young stromal cells, which essentially showed an increase in the number of CFU-pre-B cells ($P < 0.001$ in 5 μg/ml). Furthermore, TGF-β protein level in the supernatant of cultured senescent stroma cells was evaluated by enzyme-linked immunoabsorbent assay, but surprisingly, it was found that TGF-β concentration was significantly lower than that of cultured young stromal cells. Thus, TGF-β activity was assumed to decline particularly in a senescent stroma, which means a distinct difference between the senescent suppression of B lymphopoiesis and secondary B lymphocytopenia. Concerning proliferative signaling, on the other hand, the level of *IL-7* gene expression in cells from freshly isolated BM decreased significantly with age. Therefore, the acceleration of proliferative signaling and the deceleration of suppressive signaling may both be altered and weakened in a senescent stroma (i.e., homeosupression). Exp Biol Med 229:494–502, 2004

Key words: aging; B-lymphopoiesis; interleukin-7; transforming growth factor-β; senescence-accelerated mice; homeosuppression

This work was supported by a Grant-in-Aid (No. 13670236) for Scientific Research C from the Japan Society for the Promotion of Sciences.

[1] To whom requests for reprints should be addressed to Center for Biological Safety and Research, National Institute of Health Sciences, 1-18-1 Kamiyohga, Setagayaku, Tokyo 158–8501, Japan. E-mail: tohru@nihs.go.jp

Received August 1, 2003.
Accepted March 1, 2004.

1535-3702/04/2296-0001$15.00

Introduction

Aging is accompanied by changes in the immune system, leading to a decrease in the overall cellular and humoral responsiveness (1). Because the most marked age-associated change in the immune system is the rapid involution of the thymus after puberty, most of the decline in humoral immunity has been attributed to changes in the T-cell compartment rather than to an intrinsic primary B cell

deficit. Consequently, attention has been focused on age-associated changes in T lymphocytes and their functions (2). However, it has recently been clarified that there are also deficiencies in B cell development in the bone marrow (BM) of aged animals (3–6). Alterations in B cell development may include both the skewing of *V*-gene utilization, particularly in cells responsive to phosphoryl choline, and the decrease in the generation of various developmental B cell subsets. The altered representation of these subsets appears to be a consequence of a developmental arrest of the maturation of pro-B cells and the earliest stage of surface Ig-positive cells (7). Age-related changes in the B cell development may account for the deterioration of the immune system in senescent mice.

B lymphopoiesis is suppressed during senescence not only in mice but also in humans. A decrease in interleukin-7 (IL-7) production by stromal cells and a simultaneous reduction in B lymphocyte reactivity to IL-7 are considered as a possible background for this negative senescent regulation. Furthermore, in addition to senescence, B cells were noted to be regulated by two pathways not only for IL-7 but also for transforming growth factor-β (TGF-β) in regular mice; that is, not only the downregulation of the former but also the upregulation of the latter simultaneously play a role in suppression regulation (8). This is in good agreement with the observation that the supplementation of IL-7 could not compensate for the B cell suppression. In this study, possible senescence-associated alterations in the productions of IL-7 and TGF-β are examined in senescence-accelerated mice (SAMs).

Senescence-accelerated mice provide a unique model system for studying senescence or aging in higher organisms, because they exhibit a marked acceleration of aging, which has been confirmed to be the same manner as that observed in the regular mice. Senescence-accelerated mice are characterized by the early onset of aging (mean life span of 40 weeks under conventional conditions), loss of general behavioral activity, increased skin coarseness, and spinal lordokyphosis (9). Because the number of splenic cells starts to decrease at approximately 30 weeks old, the SAMs used were, in general, 30 weeks old or slightly older. Although one must carefully interpret the results of studies using SAMs because the mechanism of "accelerated aging" may not be associated with that of "normal aging," results of previous studies conducted by other researchers and ourselves indicate that SAMs are a suitable model for predicting the possible mechanism of aging in hematopoietic systems (10–14).

The purposes of this study are to confirm the status of B lymphopoiesis in SAMs compared with that in other regular strains and to elucidate the mechanism of age-related changes in B lymphopoiesis in SAMs. Here, we examined age-related changes in the number and function of B cell progenitors in the BM and their supportive microenvironment.

Materials and Methods

Mice. A senescence-prone substrain of the AKR/J mouse, SAMs/P-1 (9), from The Jackson Laboratory in Bar Harbor, ME, was kindly provided by Dr. Toshio Takeda, Emeritus, the Chest Disease Research Institute, Kyoto University. The mice were bred and maintained at the experimental animal facility of the National Institute of Health Sciences under pathogen-free conditions. Male SAMs designated as "young (8–12 weeks old)" or "senescent (30–36 weeks old)" were used in the present study; these ages were selected because the number of splenic cells and/or hemopoietic progenitor cells start to decrease at approximately 30 weeks of age (11).

Preparation of BM Cells. The BM cell suspensions were prepared by repeatedly flushing the cells from femurs and dispersing them by trituration through a 23-gauge hypodermic needle with the Iscove-modified Dulbecco medium (IMDM; Invitrogen Corp., Carlsbad, CA) or RPMI 1640 medium (Invitrogen).

***In Vitro* Colony Assays.** Colony-forming unit pre-B (CFU-pre-B) cells were assayed by suspending mononuclear cells in 1-ml aliquots of the recombinant IL-7 (rIL-7)–supplemented MethoCult M 3630 medium (Stem Cell Technologies Inc., Vancouver, Canada) in 35-mm, plastic petri dishes. Femoral BM cells from three mice per group were pooled and assayed. A MethoCult M 3630 medium consisting of 1 ml of the semisolid IMDM medium containing 1% methylcellulose, 30% fetal bovine serum (FBS; HyClone Laboratories, Inc., Logan, UT), 0.1 m*M* 2-mercaptoethanol (2-ME), 2 m*M* L-glutamine, and 10 ng/ml of rIL-7 (R&D Systems, Inc., Minneapolis, MN) was used. Granulocyte-macrophage colony-forming units (GM-CFUs) were assayed by suspending mononuclear cells in the alpha medium containing 1% methyl cellulose, 30% FBS, 1% bovine serum albumin, 1 m*M* 2-ME, and 10 ng/ml of granulocyte-macrophage colony-stimulating factor (Genzyme, Cambridge, MA) and plating 1-ml aliquots in 35-mm, plastic dishes. Both CFU-pre-B cells and GM-CFUs in culture plates in triplicate were incubated at 37°C in a fully humidified atmosphere of 5% carbon dioxide in air. Aggregates of 50 or more cells in 7-day cultures were counted as colonies. Aggregates ranging from 10 to 49 cells were counted as clusters.

Co-culture of Stromal Monolayers and Pro-B/Pre-B Cell-Rich Populations. Stromal monolayers were prepared by culturing BM cells derived from young or senescent SAMs at 1×10^6/ml in 96-well Coster 3596 or 24-well Falcon 3047 flat-bottomed plates in 0.2 or 1 ml of the RPMI 1640 medium supplemented with 20% FBS. Confluent adherent layers were formed after 7 days. To obtain pro-B/pre-B cell-rich populations, the bulk culture of pooled BM cells from young SAMs stimulated with rIL-7 was performed as described previously (4). Briefly, BM cells from young SAMs were cultured at 1×10^6 cells/ml in RPMI 1640 supplemented with 20% FBS, 2×10^{-5} *M*

2-ME, 1% L-glutamine, and 2 ng/ml of murine rIL-7 (Genzyme) and plated in six-well Coster 3516 culture trays. Nonadherent cells were harvested after 4 days of culture. This bulk culture provided a highly rich (>10-fold) source of IL-7–responsive $B220^+$, $CD43^+$, IgM^-, pro-B/pre-B cells (data not shown). Pro-B/pre-B cell-rich populations were suspended at 5×10^4/ml in RPMI 1640 supplemented with 20% FBS, 2×10^{-5} *M* 2-ME, 1% L-glutamine, and 1 ng/ml of murine rIL-7. Aliquots (0.1 or 1.0 ml) of this cell suspension were added to established stromal cell monolayers in 96- and 24-well flat-bottomed trays, respectively, and co-cultured at 37°C in a fully humidified atmosphere of 5% carbon dioxide in air. Nonadherent cells were harvested after 3 days, counted, and cloned using the CFU-pre-B colony assay system.

Extraction of Total RNA and Polymerase Chain Reaction (PCR). Total RNA was extracted from BM cells using the TRIsol reagent (Invitrogen) according to the manufacturer's instructions. First, messenger RNA (mRNA) was reverse transcribed using superscript (Life Technologies, Grand Island, NY) and random hexamers. Next, PCR amplification of complementary DNA (cDNA) was performed with the graded dilution of cDNA for semiquantitative evaluation of IL-7 and glyceraldehyde-3-phosphate dehydrogenase (GAPDH) expression under the following conditions: IL-7 cDNA, 95 °C for 1 min, 55°C for 2 mins, and 72°C for 3 mins for 35 cycles; and GAPDH cDNA, 94°C for 30 secs, 60°C for 30 secs, and 72°C for 1 min for 20 cycles. Murine IL-7 and GAPDH primers were synthesized based on a published cDNA sequence (15):

IL-7 (sense) 5'-GCCTGTCACATCTGAGTGGC-3'

IL-7 (antisense) 5'-CAGGAGGCATCCAG-GAACTTCTG-3'

GAPDH (sense) 5'-TGAAGGTCGGTGTGAACG-GATTTGGC-3'

GAPDH (antisense) 5'-CATGTAGGCCATGAGGTC-CACCAC-3'

The expected amplified PCR products were 496 and 982 base pairs long for IL-7 and GAPDH, respectively. The PCR products were photographed using the Bio-Rad 2000 gel documentation system (Bio-Rad Laboratories, Hercules, CA), and intensities of expressions were evaluated by ImageGauge version 3.11 (Science Lab 98 for Windows; Fuji Film, Tokyo, Japan). In this experiment, GAPDH expressions were not altered among the experimental groups.

Effect of Anti–TGF-β Antibody on Growth of Pro-B/Pre-B Cell-Rich Population Co-Cultured with Stromal Cells. To examine the effect of TGF-β produced by stromal cells on the growth of pro-B/pre-B cells, a neutralizing monoclonal antibody (mAb) to TGF-β (mouse IgG_1 isotype, R&D Systems) at dilutions ranging from 1–10 μg/ml was added to the co-culture system. The mouse IgG_1 isotype (R&D Systems) was used as mock control. The number of nonadherent cells in the co-cultures was determined 3 days later.

Determination of Level of TGF-β Protein Produced by Cultured Stromal Cells. Stromal monolayers were prepared by culturing BM cells from young and senescent SAMs at 1×10^6/ml in 24-well Falcon 3047 flat-bottomed plates in 1 ml of the RPMI 1640 medium supplemented with 20% FBS. Confluent adherent layers were obtained after 7 days. The supernatant in the culture plates was removed; and then 1 ml of RPMI 1640, supplemented with 20% FBS, 2×10^{-5} *M* 2-ME, and 1% L-glutamine were added to the culture plates. The culture medium was collected after 7 days of culture and was used for the determination of the level of the TGF-β protein produced by stromal cells. The TGF-β concentration in the culture medium was determined using a TGF-β–specific enzyme-linked immunoabsorbent assay (ELISA) kit (R&D Systems) according to the manufacturer's instructions. All the samples were assayed in triplicate. The samples were acid activated (16) by adding 1/5 vol of 1 *N* hydrochloride at room temperature and neutralized after 10 mins by adding of 1/5 vol of 1.2 *N* NaOH in 0.5 *M* HEPES, and the mixture was diluted with the same volume of calibrator diluents in the ELISA kit.

Statistical Analysis. Data were analyzed using the analysis of variance (ANOVA). Values were considered significantly different at $P < 0.05$.

Results

Decrease in Number of B Cell Progenitors (Pre-B Cells). Age-related changes in the numbers of B lymphocytes and hematopoietic progenitors differ from each other. Table 1 summarizes the results of the triplicate experiments. The number of femoral GM-CFU cells from 30-week-old and 36-week-old senescent mice assayed on the basis of their colony-forming ability increased to 112% and 109%, respectively, that of GM-CFU from 12-week-old mice. In contrast, the CFU-pre-B colony assay, using Day 7 B cell colonies as the end point, was used to determine the number of IL-7–responsive B cell progenitors in young and senescent BM cells. The numbers of femoral CFU-pre-B cells from 30-week-old and 36-week-old mice decreased to 75.7% and 65.0%, respectively, that from 12-week-old mice. Furthermore, the decrease in the number of CFU-pre-B cells from femoral BM in senescent mice could not be counteracted by increasing IL-7 concentration in the culture medium 4-fold or by extending the culture period (data not shown).

Significant Decrease in Number of Large Pre-B Colonies. Among B cell colonies of various sizes, we noted that the number of relatively larger B cell colonies decreased significantly with aging (Fig. 1). The number of cells per colony ranged from 50–5000. Therefore, CFU-pre-B cell colonies in Table 1 were categorized according to their size, namely, small (50–200 cells), intermediate (201–

Table 1. Age-Related Changes in Number of Hematopoietic Progenitor Cells in Senescence-Accelerated Mice[a]

	Mean ± SEM of triplicate experiments (%)		
	12-week-old mice	30-week-old mice	36-week-old mice
Femoral GM-CFU cells	72,762 ± 672	81,250 ± 2811 (112%)	79,058 ± 4763 (109%)
Femoral CFU-pre-B cells	13,868 ± 516	10,505 ± 1083* (75.7%)	9017 ± 220** (65.0%)

[a] GM-CFU, granulocyte-macrophage colony-forming unit; CFU-pre-B, colony-forming unit pre-B.
* $P < 0.05$; ** $P < 0.001$.

3000), and large (>3000 cells). As shown in Figure 1, the numbers of large, intermediate, and small B cell colonies for all groups decreased with age (58.3% for large colonies, 75.8% for intermediate colonies, 78.4% for small colonies in 30-week-old mice relative to those in 12-week-old mice; 22.1% for large colonies, 52.0% for intermediate colonies, and 76.5% for small colonies in 36-week-old mice relative to those in 12-week-old mice). The decrease in the numbers was statistically most significant for large colonies in 30- and 36-week-old mice relative to those to 12-week-old control ($P < 0.001$ and $P < 0.005$, respectively) and also for intermediate colonies in 36-week-old mice relative to those in 12-week-old control ($P < 0.05$).

Decrease in IL-7 Expression Level in BM. As observed in the regular senescent mice, the number of pre-B cell progenitors also decreased in SAMs. Therefore, the expression level of IL-7, which is known to be a pre-B cell stimulator, was evaluated in BM cells. IL-7 expression level decrease during senescence (17–19). In this study, IL-7 mRNA expression level was evaluated by reverse transcriptase (RT)–PCR. The BM stromal cell–derived IL-7 is a positive regulator of *in vivo* B lymphopoiesis. As shown in Figure 2, the IL-7 mRNA expression level in BM cells from senescent mice was 6.2% that from young mice. These findings are comparable to those in the literature (17–19). Further experiments using SAMs were designed.

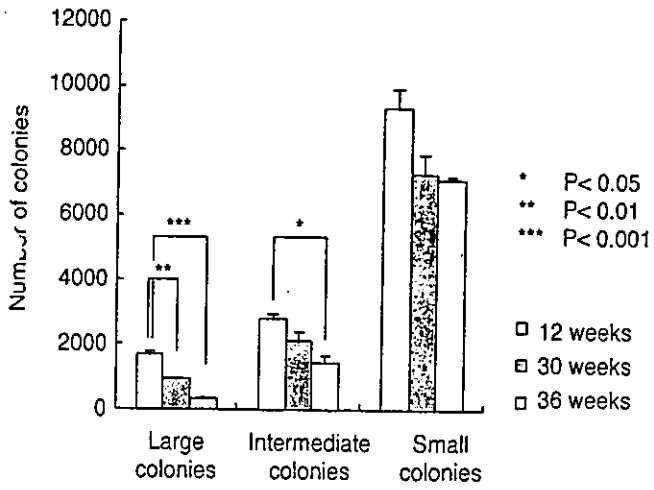

Figure 1. Age-related changes in number of B cell colonies of large, intermediate, and small sizes (mean ± SEM of three replicate experiments). Femoral bone marrow (BM) cells from three mice per group were harvested and pooled. The preparation of BM cell suspensions is described in the "Materials and Methods" section. Colony-forming unit pre-B (CFU-pre-B) cells were assayed by suspending mononuclear cells in 1-ml aliquots of the recombinant interleukin-7 (rIL-7)–supplemented MethoCult M 3630 medium (Stem Cell Technologies Inc., Vancouver, Canada) in 35-mm, plastic petri dishes. Culture plates in triplicate for CFU-pre-B cells were incubated at 37 °C in a fully humidified atmosphere of 5% carbon dioxide in air. According to the size of CFU-pre-B cell colonies shown in Table 1, colonies were categorized as follows: small (50–200 cells), intermediate (201–3000), and large (>3000 cells).

Decrease in Proliferative Capacity of B Cell Progenitors, Pre-B Cell Response to IL-7. The decrease in IL-7 expression level is also associated with the decrease in the responsiveness of pre-B cells to IL-7. To evaluate such responsiveness, we used a recloning assay to determine the proliferative capacity of the progeny of CFU-pre-B cells. Cells derived from 36 large colonies were pooled and recloned for 7 days in a semisolid medium supplemented with rIL-7. Table 2 shows the results of the recloning study. The numbers of secondary colonies, which included small (50–200 cells) and intermediate (201–3000) colonies and clusters (10–49 cells) generated from individual large primary colonies and derived from 30-week-old and 36-week-old femoral BMs, decreased significantly to 69.0% and 2.7%, respectively, that of secondary colonies grown from large primary colonies derived from 12-week-old femoral BM. Furthermore, cells from small primary colonies derived from either young or senescent mouse BM formed no secondary colonies. In B lymphopoiesis, unlike in the case of myelogenous progenitors, the results indicate that the responsiveness of CFU-pre-B cells to IL-7 decreases with age.

Decrease in Maintenance Capacity of Stromal Cells for B Lymphopoiesis. Although the pre-B progenitor cells were altered during senescence, a decrease in the maintenance capacity of stromal cells for B cell lineages may also be of importance in association with hematopoietic senescence (17, 18, 20). Using a co-culture system in 24-well flat-bottomed trays, we determined whether the capacity of stromal cells to support B lymphopoiesis is altered with age. Interestingly and unexpectedly, the number of lymphocytes recovered from the coculture of pro-B/pre-B cells with young stromal cells was significantly lower than that recovered from senescent stromal cells (Fig. 3A). In contrast, the total number of CFU-pre-B cells recovered from the co-culture with young stromal cells was significantly higher than that recovered from the co-culture with senescent stromal cells (Fig. 3B).

Decrease in TGF-β Production by Senescent Stromal Cells. On the basis of the above-mentioned co-

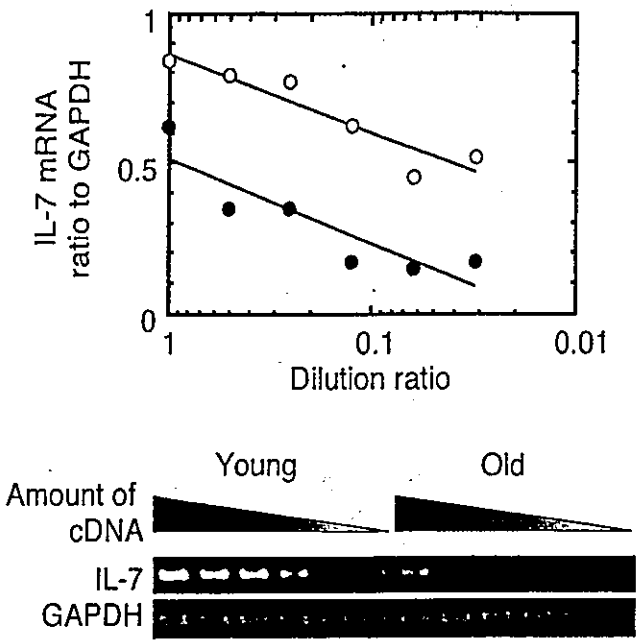

Figure 2. Expression level of interleukin-7 (IL-7) messenger RNA (mRNA) in bone marrow (BM) cells freshly isolated from young and old senescence-accelerated mice (mean ± SEM of three replicate experiments). Vertical bars for SEM are within the symbols. Total RNA was extracted from BM cells using the TRIsol reagent (Invitrogen Corp., Carlsbad, CA) according to the manufacturer's instructions. The extracted mRNA was reverse transcribed using Superscript (Life Technologies, Grand Island, NY) and random hexamers. The reverse-transcribed complementary DNAs (cDNAs) are then amplified by polymerase chain reaction (PCR) using specific primers for murine IL-7 and glyceraldehyde-3-phosphate dehydrogenase (GAPDH). The conditions and primer sequences used for the PCR amplification of cDNAs are shown in the "Materials and Methods" section of reference 15. The expected amplified PCR products were 496 and 982 base pairs long for IL-7 and GAPDH, respectively. In this experiment, GAPDH expressions were not altered among the experimental groups.

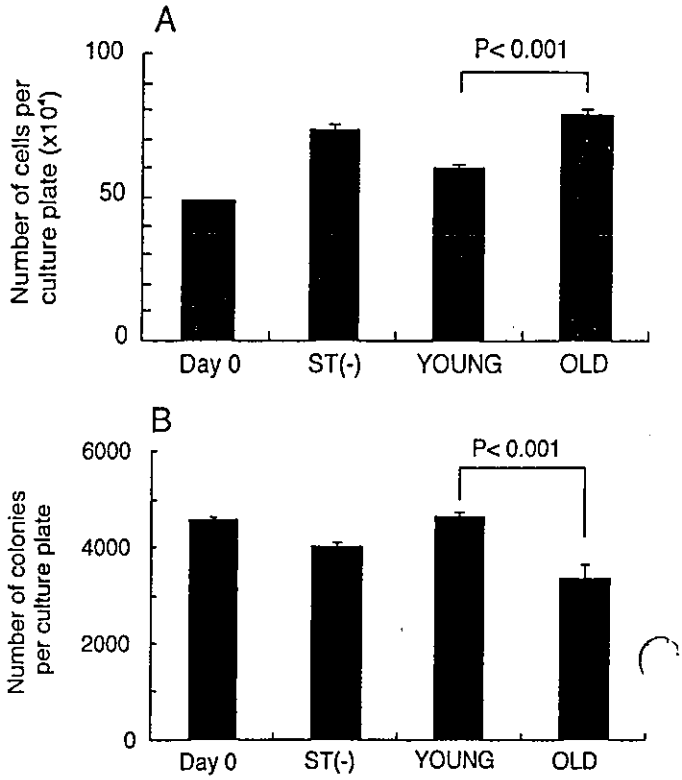

Figure 3. (A) Co-culture of pro-B/pre-B cell-enriched populations with stromal cells: change in the number of nonadherent cells (mean ± SEM of three replicate experiments). (B) Co-culture of pro-B/pre-B cell-rich populations with stromal cells: change in total number of CFU-pre-B cells (mean ± SEM of three replicate experiments). Stromal monolayers were prepared by culturing bone marrow (BM) cells from young or senescent senescence-accelerated mice (SAMs) at 1 × 10^6/ml in 96-well Coster 3596 or 24-well Falcon 3047 flat-bottom plates in 0.2 or 1 ml of the RPMI 1640 medium supplemented with 20% fetal bovine serum. Confluent adherent layers were formed after 7 days. To obtain Pro-B/pre-B cell-rich populations (>10-fold) (i.e., interleukin-7 [IL-7]–responsive B220$^+$, CD43$^+$, IgM$^-$, pro-B/pre-B cells), pooled BM cells from young SAMs stimulated with recombinant IL-7 were cultured, as described in the "Materials and Methods" section (4). Nonadherent cells were harvested and counted. Day 0 indicates nonadherent cell number at the beginning of co-culture; ST (-), nonadherent cell number after culture with IL-7 alone; YOUNG, nonadherent cell number after co-culture with young stromal cells in the presence of IL-7; OLD, nonadherent cell number after co-culture with senescent stromal cells in the presence of IL-7.

culture data, we propose a hypothesis that the CFU-pre-B inhibitory activity of BM cells may reside predominantly in young stromal cells rather than in senescent stromal cells. Because stromal cells produce BM-derived TGF-β (21) and are also a negative regulator of B lymphopoiesis (22–24), we investigated whether TGF-β production by stromal cells is reduced with age. Figure 4 shows percent changes in the number of the same seeded BM cells cocultured with young stromal cells (open circles) or senescent stromal cells (closed circles) in 96-well flat-bottomed trays after adding a graded dose of a neutralizing mAb to TGF-β. The high-dose group (10 μg/ml and more; data not shown) exhibited a toxic effect, but the lower-dose group showed a significant difference of responses between the young and senescent groups, implying that the proliferation of the senescent

Table 2. Secondary B Cell Colonies Derived From One Large Colony-Forming Unit B Cell Colony[a]

Donor mouse age (week)	Mean ± SEM of triplicate experiments					
	Large	Intermediate	Small	Cluster	No. of total colonies[b] (with cluster)[c]	% to a/% to b
12	ND	1.4 ± 0.6	5.8 ± 0.7	7.2 ± 0.6	7.2 ± 0.6 (14.4 ± 1.0)	100%/100%
30	ND	ND	2.3 ± 0.5	7.4 ± 1.7	2.3 ± 0.5* (9.7 ± 1.4)**	24%/69%
36	ND	ND	ND	0.4 ± 0.2	ND (0.4 ± 0.2)**	—/2.7%

[a] Percentages for 30-week-old or 36-week-old mice compared with 12-week-old mice are shown in parentheses. ND, not detected.
[b] Number of total colonies by large, intermediate, and small B cell colonies without clusters.
[c] Number of total colonies with clusters.
* $P < 0.005$; ** $P < 0.01$.

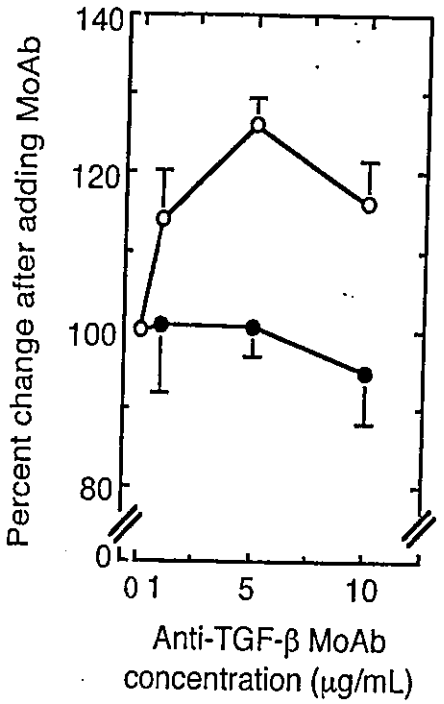

Figure 4. Effect of neutralizing anti–transforming growth factor-β (TGF-β) monoclonal antibody (mAb) on proliferation of pro-B/pre-B cells from young senescence-accelerated mice co-cultured with femoral stromal cells from young mice (open circles) and those from senescent mice (closed circles). The effect of TGF-β on the growth of pro-B/pre-B cells was evaluated on the basis of the number of nonadherent cells after the supplementation of the neutralizing antibody to TGF-β (mouse IgG_1 isotype: R&D Systems, Inc., Minneapolis, MN) at dilutions ranging from 1–10 μg/ml to the coculture system. The mouse IgG_1 isotype (R&D Systems) was used as the mock control. The senescent group shows no substantial rescue effect of mAb, whereas the young group shows significant rescue effect of mAb by repeated-measure analysis of variance testing (P = 0.0111). (Vertical bars indicate SEM of triplicate experiments).

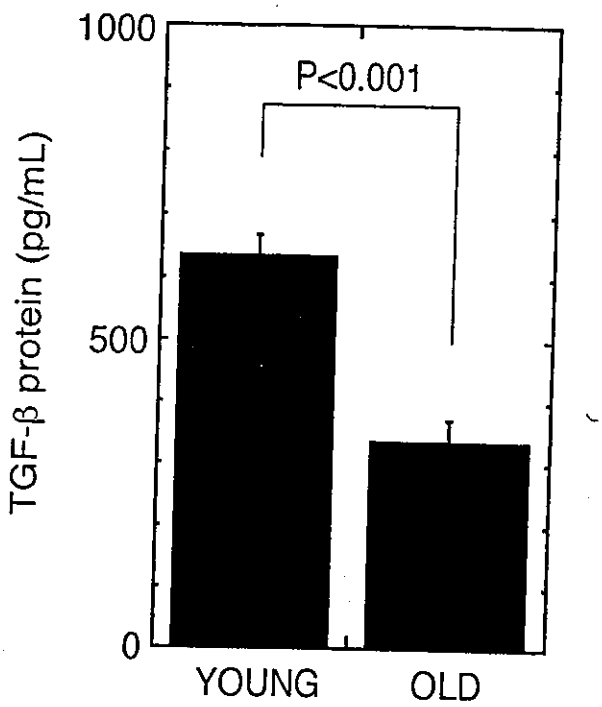

Figure 5. Transforming growth factor-β (TGF-β) protein level in the supernatant of cultured stromal cells from young and senescent senescence-accelerated mice (SAMs) (mean ± SEM of three replicate experiments). Stromal monolayers were prepared by culturing bone marrow (BM) cells from young or senescent SAMs at 1×10^6/ml in 24-well Falcon 3047 flat-bottom plates in 1 ml of the RPMI 1640 medium supplemented with 20% fetal bovine serum (FBS). Confluent adherent layers were formed after 7 days. The supernatant of culture plates was removed, 1 ml of RPMI 1640 was supplemented with 20% FBS, and 2×10^{-5} M 2-ME and 1% L-glutamine were added to the culture plates. The culture medium was collected after culture for 7 days and was used for determination of the level of the TGF-β protein produced by stromal cells. The TGF-β concentration in culture medium was determined using a TGF-β–specific enzyme-linked immunoabsorbent assay kit.

group was unexpectedly not recovered by the neutralizing antibody, whereas (although it was not expected) the proliferation of the young group was prominently recovered at 1- and 5-μg/ml doses (statistical significance, $P < 0.001$ in the group of 5 μg/ml). Thus, despite the prominent decrease in IL-7 expression level and in the biological activity of IL-7 in the BM, TGF-β production seemed to have unexpectedly decreased in the senescent group. To confirm the decrease in TGF-β production by stromal cells with age, we directly measured TGF-β protein level in the supernatant of cultured stromal cells derived from young and senescent SAMs using ELISA. Figure 5 shows that the TGF-β protein level in the supernatant of cultured senescent stromal cells is markedly lower than that of cultured young stroma, thus implying that TGF-β production by stromal cells decreases with age (634.0 ± 36.0 vs. 337.0 ± 37.9, young and old, respectively, $P < 0.001$).

Discussion

It has long been questioned whether age-related alterations in B lymphopoiesis are mainly due to a functional impairment of B cell precursor cells or due to that of senescent stromal cells. Several studies showed steady-state B lymphopoiesis and focused on the decrease in B cell production due in part to the decreased IL-7 responsiveness (25, 26). Indeed, our initial experiments demonstrated that the numbers of femoral CFU-pre-B cells (3-6), particularly those forming large colonies, decrease with age, suggesting that age-related alterations of B lymphopoiesis seem to be based on the quality of B cell precursors (Table 1 and Fig. 1).

The expression level of IL-7, a pre-B cell stimulator, was evaluated in BM cells, because IL-7 production decreases during senescence (17–19). Mice in which the *IL-7* gene has been knocked out manifest a prominent decrease in the number of pre-B lymphocytes and a severe impairment in capacity for self-renewal in the pre-B cell compartment, even though the number of pro-B cells appears to be normal. Phenotypically, age-related changes seem closer to the changes in the B lymphopoiesis observed in aged mice (27). Our data showed that the IL-7 mRNA expression level in freshly isolated BM cells decreases with age (Fig. 2). We attempted to measure IL-7 expression level only in freshly isolated BM cells and BM stromal cells, because the expression of IL-7 is easily upregulated

immediately after the start of culture. Because of the limited materials for ELISA, protein expression level was not determined. These findings are consistent with those of Updyke *et al.* (17), who reported that the relative quantity of the IL-7 protein released into the medium for long-term B cell culture decreases with age. A study by Stephan *et al.* (18) suggested that the age-related decrease in the function of BM cells is associated with the impaired release of IL-7. Interestingly, a novel mutant mouse model of aging, *klotho*, was reported to exhibit a similar significant decrease in the level of *IL-7* gene expression in freshly isolated BM cells as determined by RT-PCR analysis (19); the mouse initially exhibits multiple disorders that resemble various aging phenotypes. Based on the findings by other researchers and ourselves, it seems likely that IL-7 production by BM stromal cells decreases with age. As seen in Figures 1–4, comparable results were obtained in reports available in the literature; hence, the present findings obtained through the experiment using SAMs may be applicable to the analysis of natural aging in regular mice.

Next, we demonstrated that the production of TGF-β by marrow stromal cells decreased with age, although the mechanism underlying this phenomenon is not yet known. Young stromal cells inhibited B cell proliferation in the co-culture system, and this inhibition was reversed by treatment with antibodies to TGF-β. The results of the co-culture system demonstrated that significantly fewer lymphocytes could be recovered from the co-culture system with young stromal cells than with senescent stromal cells; conversely, a significantly higher number of CFU-pre-B cells is maintained in the co-culture system with young stromal cells than with senescent stromal cells (Fig. 3A and B). Moreover, the neutralizing antibody to TGF-β restored the proliferative capacity of pro-B/pre-B cells co-cultured with young stromal cells but not that of those co-cultured with senescent stromal cells (Fig. 4). Furthermore, the TGF-β protein level in supernatant of cultured senescent stromal cells is markedly lower than that of young stromal cells (Fig. 5). These results imply that senescent stromal cells are not capable of producing TGF-β. These data agree with those reported by Dubinett *et al.* (28) that IL-7 downregulates both mRNA expression and protein production of TGF-β by murine macrophages. Thus, it seems unlikely that exogenous IL-7 added to our co-culture system would induce TGF-β production by stromal cells derived from a young stroma. Furthermore, Gazit *et al.* (29) have recently reported that fibroblast CFU (CFU-F) isolated from senescent mice produces less TGF-β *in vitro* than CFU-F from young mice and that the matrix of long bones of senescent mice contains less TGF-β than that of young mice. These data suggest that the production of the CFU-pre-B cell regulator TGF-β by stromal cells may decrease with age. Consequently, CFU-pre-B cells co-cultured with senescent stromal cells may proliferate and/or differentiate more rapidly than CFU-pre-B cells co-cultured with young stromal cells in the presence of IL-7.

In the present study, we observed that the CFU-pre-B cell number in the BM decreased with age, whereas, as we have observed previously (13), the total number of splenic B cells remained relatively unchanged. These findings are consistent with those observed in other murine strains by other researchers (3–6) and have been considered to be mediated by a decrease in B lymphocyte production in the BM and increased longevity of mature B cells (30). Furthermore, our data revealed an intrinsic defect in the B-progenitor-cell response to IL-7, as well as an age-related impaired production of not only IL-7 but also TGF-β by stromal cells. In SAMs, the arrest of pro-B cell maturation with advanced aging was evidently associated with the decrease in the number of pre-B cells. This may be explained by the coexistence of an intrinsic defect in the B-progenitor-cell response to IL-7 (i.e., pre-B cells and more immature pro-B cells); this interpretation is in good agreement with previous reports (6). Moreover, a decrease in IL-7 production by stromal cells during aging was confirmed (Fig. 2), which is evident in regular mice (17, 18).

The present study revealed that senescent B lymphopoiesis is suppressed, the background mechanism of which is unlikely different from mechanical B cell damage and its acute responses. Although B cell damage may be based on a positive circuit (i.e., an increase in IL-7 production associated with a decrease in TGF-β production) (28, 31, 32), our present data clearly show that TGF-β production is rather suppressed despite the prominent decrease in IL-7 production. Such homeostatic B lymphopoiesis balanced at the lower level may be a prominent characteristic of the basic mechanism of B lymphopoietic senescence, although the details of this mechanism are as yet unknown.

Another objective of our current study is to address the issue of using SAMs as an experimental mouse model for predicting the possible basic mechanism of senescence and B lymphopoiesis during aging. Aging is a physiological process and is likely controlled by a combination of many different factors. Whether the determinant of accelerated aging in SAMs is the same as that of normal aging in mice remains to be elucidated. However, the determinant factors for aging of an organism are, at present, poorly understood. Thus, different experimental approaches using animal models such as SAMs may provide an insight into such factors, because the study of abnormal systems has often led to the clarification of how a normal system functions.

Our present study, performed using SAMs and focusing on the quantity and quality of B lymphopoietic progenitor cells, suggests age-related alterations in lymphopoietic progenitor cells. Among them, the changes shown in Tables 1 and 2 and Figure 1 are essentially identical to those observed in regular mouse strains as previously reported. Namely, the decreased IL-7 responsiveness of BM cells from aged mice appears to be associated with both the decrease in the number of IL-7–responsive cells and the decrease in colony size and to correlate with findings in other strains (3–6). Furthermore, the number of secondary

colonies generated by the progeny of CFU-pre-B cells derived from large primary colonies was significantly smaller for the BM of senescent mice than for that of young mice (Table 2). Note that there seems to be an almost complete arrest in the production of secondary CFU-pre-B colonies from 36-week-old mice (Table 2), whereas comparable primary BM cells produced the same amount of GM-CFU (109%) from 12-week-old mice, and 65.0% of CFU-pre-B colonies was maintained (Table 1) in 12-week-old mice. The decrease in the number of secondary colonies was prominently observed in the most senescent age group (i.e., 36 weeks old) at the level of "cluster," because there seems to be a split between the time to senescence for spleen atrophy and that for substantial hemopoietic arrest in *in vitro* colonization. Stephan *et al.* (25) reported that a small percentage of BM pro-B cells from aged mice undergo cell cycle and that a large percentage of these cells enter G0/G1 after stimulation with IL-7, suggesting an impairment or delay in their ability to undergo cell division after IL-7 timulation. The surrogate light chain is a component of the pre-B cell receptor, which is critical for Ig-variable heavy chain selection, cellular proliferation, and survival in the pre-B stage. Sherwood *et al.* (26) and Frasca *et al.* (33) reported that surrogate L chain mRNA and protein levels in IL-7–expanded B cell precursors decrease with age, which is associated with decreased protein levels of the E2A-encoded transcription factors, E47 and E12 (33). Based on these results, impairment in the IL-7 receptor function and its signal transduction in pro-B/pre-B cells may underlie the decrease in B cell production with age. It seems likely that the reduced generation of secondary colonies may be due in part to the deterioration of the proliferative capacity of B-cell progenitors from senescent mice in response to IL-7 rather than to the exclusive differentiation of B-cell progenitors to mature B cells in response to IL-7. In this regard, senescent changes observed in B lymphopoiesis in SAMs may be assumed to be identical to those reported in regular mice.

We thank Dr. Yukio Kodama, Ms. Erika Tachihara, Ms. Yoshiko Usami, and Ms. Yasuko Shinzawa for assistance in the maintenance of SAMs at the experimental animal facilities and Ms. Noriko Katsu and Ms. Chiaki Kimura for secretarial help in the preparation of the manuscript.

1. Hodes RJ. Aging and the immune system. Immunol Rev 160:5–8, 1997.
2. Ghia P, Melchers F, Rolink AG. Age-dependent changes in B lymphocyte development in man and mouse. Exp Gerontol 35:159–165, 2000.
3. Zharhary D. Age-related changes in the capability of the bone marrow to generate B cells. J Immunol 141:1863–1869, 1988.
4. Riley RL, Kruger MG, Elia J. B cell precursors are decreased in senescent BALB/c mice, but retain normal mitotic activity in vivo and in vitro. Clin Immunol Immunopathol 59:301–313, 1991.
5. Jonsson JI, Phillips RA. Interleukin-7 responsiveness of B220+ B cell precursors from bone marrow decreases in aging mice. Cell Immunol 147:267–278, 1993.
6. Stephan RP, Sanders VM, Witte PL. Stage-specific alterations in murine B lymphopoiesis with age. Int Immunol 8:509–518, 1996.
7. Klinman NR, Kline GH. The B-cell biology of aging. Immunol Rev 160:103–114, 1997.
8. Tang J, Nuccie BL, Ritterman I, Liesveld JL, Abboud CN, Ryan DH. TGF-beta down-regulates stromal IL-7 secretion and inhibits proliferation of human B cell precursors. J Immunol 159:117–125, 1997.
9. Takeda T, Hosokawa M, Takeshita S, Irino M, Higuchi K, Matsushita T, Tomita Y, Yasuhira K, Hamamoto H, Shimizu K, Ishii M, Yamamuro T. A new murine model of accelerated senescence. Mech Ageing Dev 17:183–194, 1981.
10. Izumi-Hisha H, Ito Y, Sugimoto K, Oshima H, Mori KJ. Age-related decrease in the number of hemopoietic stem cells and progenitors in senescence accelerated mice. Mech Ageing Dev 56:89–97, 1990.
11. Tsuboi I, Morimoto K, Horie T, Mori KJ. Age-related changes in various hemopoietic progenitor cells in senescence-accelerated (SAM-P) mice. Exp Hematol 19:874–877, 1991.
12. Sakuma A, Tsuboi I, Morimoto K, Horie T, Sugimoto K, Mori KJ. Age-related decreases in the reconstituting ability of hemopoietic cells and the ability of hemopoietic microenvironment to support hemopoietic reconstitution in senescence accelerated (SAM-P) mice. Mech Ageing Dev 73:127–135, 1994.
13. Saitoh T, Morimoto K, Kumagai T, Tsuboi I, Aikawa S, Horie T. Comparison of erythropoietic response to androgen in young and old senescence accelerated mice. Mech Ageing Dev 109:125–139, 1999.
14. Kumagai T, Morimoto K, Saitoh T, Tsuboi I, Aikawa S, Horie T. Age-related changes in myelopoietic response to lipopolysaccharide in senescence-accelerated (SAM) mice. Mech Ageing Dev 112:153–167, 2000.
15. Yamamoto H, Hatano M, Iitsuka Y, Mahyar NS, Yamamoto M, Tokuhisa T. Two forms of Hox11 a T cell leukemia oncogene, are expressed in fetal spleen but not in primary lymphocytes. Mol Immunol 32:1177–1182, 1995.
16. Lawrence DA, Pircher R, Jullien P. Conversion of a high molecular weight latent beta-TGF from chicken embryo fibroblasts into a low molecular weight active beta-TGF under acidic conditions. Biochem Biophys Res Commun 133:1026-10-34, 1985.
17. Updyke LW, Cocke KS, Wierda D. Age-related changes in production of interleukin-7 (IL-7) by murine long-term bone marrow cultures (LTBMC). Mech Ageing Dev 69:109–117, 1993.
18. Stephan RP, Reilly CR, Witte PL. Impaired ability of bone marrow stromal cells to support B-lymphopoiesis with age. Blood 91:75–88, 1998.
19. Okada S, Yoshida T, Hong Z, Ishii G, Hatano M, Kuro OM, Nabeshima Y, Tokuhisa T. Impairment of B lymphopoiesis in precocious aging (klotho) mice. Int Immunol 12:861-871, 2000.
20. Li F, Jin F, Freitas A, Szabo P, Weksler ME. Impaired regeneration of the peripheral B cell repertoire from bone marrow following lymphopenia in old mice. Eur J Immunol 31:500-505, 2001.
21. Nemunaitis J, Tompkins CK, Andrews DF, Singer JW. Transforming growth factor beta expression in human marrow stromal cells. Eur J Haematol 46:140–145, 1991.
22. Lee G, Namen AE, Gillis S, Ellingsworth LR, Kincade PW. Normal B cell precursors responsive to recombinant murine IL-7 and inhibition of IL-7 activity by transforming growth factor-beta. J Immunol 142:3875–3883, 1989.
23. Kincade PW. B lymphopoiesis: global factors, local control. Proc Natl Acad Sci U S A 91:2888–2889, 1994.
24. Lebman DA, Edmiston JS. The role of TGF-beta in growth, differentiation, and maturation of B lymphocytes. Microbes Infect 1:1297–1304, 1999.
25. Stephan RP, Lill-Elghanian DA, Witte PL. Development of B cells in aged mice: decline in the ability of pro-B cells to respond to IL-7 but not to other growth factors. J Immunol 158:1598–1609, 1997.
26. Sherwood EM, Xu W, King AM, Blomberg BB, Riley RL. The

reduced expression of surrogate light chains in B cell precursors from senescent BALB/c mice is associated with decreased E2A proteins. Mech Ageing Dev 118:45–59, 2000.

27. von Freeden-Jeffry U, Vieira P, Lucian LA, McNeil T, Burdach SE, Murray R. Lymphopenia in interleukin (IL)-7 gene-deleted mice identifies IL-7 as a nonredundant cytokine. J Exp Med 181:1519–1526, 1995.
28. Dubinett SM, Huang M, Dhanani S, Wang J, Beroiza T. Down-regulation of macrophage transforming growth factor-beta messenger RNA expression by IL-7. J Immunol 151:6670–6680, 1993.
29. Gazit D, Zilberman Y, Ebner R, Kahn A. Bone loss (osteopenia) in old male mice results from diminished activity and availability of TGF-beta. J Cell Biochem 70:478–488, 1998.
30. Kline GH, Hayden TA, Klinman NR. B cell maintenance in aged mice reflects both increased B cell longevity and decreased B cell generation. J Immunol 162:3342–3349, 1999.
31. Miller AR, McBride WH, Dubinett SM, Dougherty GJ, Thacker JD, Shau H, Kohn DB, Moen RC, Walker MJ, Chiu R, Schuck BL, Rosenblatt JA, Huang M, Dhanani S, Rhoades K, Economou JS. Transduction of human melanoma cell lines with the human interleukin-7 gene using retroviral-mediated gene transfer: comparison of immunologic properties with interleukin-2. Blood 82:3686–3694, 1993.
32. Fry TJ, Mackall CL. Interleukin-7: from bench to clinic. Blood 99:3892–3904, 2002.
33. Frasca D, Nguyen D, Riley RL, Blomberg BB. Decreased E12 and/or E47 transcription factor activity in the bone marrow as well as in the spleen of aged mice. J Immunol 170:719–726, 2003.

Available online at www.sciencedirect.com
SCIENCE DIRECT
Reproductive Toxicology 18 (2004) 109–120
Reproductive Toxicology
www.elsevier.com/locate/reprotox

Intrauterine position and postnatal growth in Sprague–Dawley rats and ICR mice

Tetsuji Nagao[a,*], Kazuyoshi Wada[b], Makiko Kuwagata[b], Madoka Nakagomi[a], Chiaki Watanabe[b], Shinsuke Yoshimura[b], Yoshiaki Saito[b], Kenji Usumi[b], Jun Kanno[c]

[a] Department of Life Science, Faculty of Science and Technology, Kinki University, Kowakae 3-4-1, Higashiosaka, Osaka 577-8502, Japan
[b] Safety Testing Laboratory, Hatano Research Institute, Food and Drug Safety Center, Hadano, Kanagawa, Japan
[c] Division of Cellular and Molecular Toxicology, National Institute of Health Science, Tokyo, Japan

Received 13 May 2002; received in revised form 10 September 2003; accepted 16 October 2003

Abstract

In rodents, steroid hormones are thought to be transported between adjacent fetuses, and male or female fetuses that develop in utero between female fetuses may have higher serum levels of estradiol, and lower serum levels of testosterone, relative to siblings of the same sex that develop between two male fetuses. The consequence in the variation of postnatal growth, development, and function in the intrauterine position, using various parameters such as anogenital distance, preputial separation and vaginal opening, estrous cycle, locomotor activity, and growth of reproductive organs, were examined in Sprague–Dawley rats. ICR mice were treated with 17β-estradiol before copulation and during pregnancy to address the interaction with endogenous estradiol during pregnancy. In rats, no evidence of effects of prior intrauterine position was observed for any of the parameters examined. Mouse fetal exposure via the mother to low-dose 17β-estradiol revealed no changes in the rate of postnatal growth in males and females that developed in any intrauterine position in utero. The results of this study suggested that the intrauterine position of the embryos/fetuses did not affect the postnatal growth of the reproductive organs, sexual maturation, or behavior in rats and mice.

Keywords: Intrauterine position; Postnatal growth; Sexual maturation; Behavior; Anogenital distance; Rats; Mice

1. Introduction

The development of sexually differentiated phenotypes depends upon the hormonal environment during a critical period of growth [1]. Testosterone secretion by the fetal testis causes a longer anogenital distance (AGD), seen in neonatal males, relative to females. The AGD of newborn rats, mice, and gerbils is longer in males than in females and varies as a function of the intrauterine position of the animals [1–4]. A longer AGD is associated with the presence of males on either side of the developing fetus in utero, and a shorter AGD is associated with the absence of males on either side of the developing female fetus. Females with a male fetus on only one side are immediate [4].

In all litter-bearing species that have been examined to date, the intrauterine position that a fetus occupies relative to fetuses of the same or opposite sex has profound effects on its reproductive, behavioral, and morphological traits measured during adult life [4–7]. Gerbil males and females that developed in utero between two female fetuses or two male fetuses, respectively, did not differ in relative hippocampal size [8].

The effects of intrauterine position are apparently not the result of the position itself, but rather of the movement of steroid hormones between the fetuses, and variations in the hormonal environment relative to the proximity of an individual fetus to other fetuses of the same or opposite sex [9]. Male rats located between two females had elevated serum estradiol and larger prostates than males located between two males, which had elevated serum testosterone and larger seminal vesicles [10]. The effect of intrauterine position in mice has been correlated with concentrations of steroid hormones in amniotic fluid and subsequent sexual activity [11,12].

Recently, intrauterine position has been the focus of discussions in the toxicology community because of its potential to alter the susceptibility of fetuses to endogenous hormones and endocrine disrupting chemicals [13,14]. In this regard, failure to account for intrauterine position in endocrine disrupting chemical toxicology studies could lead to false negative results, especially when adverse alterations

* Corresponding author. Tel.: +81-6-6721-2332; fax: +81-6-6723-2721.
E-mail address: tnagao@msa.kindai.ac.jp (T. Nagao).

0890-6238/$ – see front matter © 2003 Elsevier Inc. All rights reserved.
doi:10.1016/j.reprotox.2003.10.009

are produced by low doses in fetuses from only one intrauterine position [14,15]. This possibility has been raised because of investigations into estrogenic compounds in mice. In rats, consistent effects due to intrauterine position on testosterone concentrations, and therefore potential interactions with endocrine disrupting chemicals, have not been found. Howdeshell and vom Saal [16] demonstrated that the greatest response to the estrogenic chemical, bisphenol A, occurred in males and females with the highest background levels of endogenous estradiol during fetal life, due to their intrauterine position, while fetuses with the lowest endogenous levels of estradiol showed no response to maternal bisphenol A within the range of human exposure, suggesting that estrogen-mimicking chemicals interact with endogenous estrogen in altering the course of development. It has been demonstrated that 2,3,7,8-tetrachlorodibenzo-*p*-dioxin interacted with endogenous estradiol to disrupt prostate gland morphogenesis in male rat fetuses [17].

The objectives of this study were to determine the effects of intrauterine position, under normal physiological conditions, on the development of rat offspring, as well as sexual maturation, estrous cycle, behavior, and reproductive organ development. Another objective of this study was to determine whether the intrauterine position of mouse fetuses, which is related to background levels of estradiol and testosterone, would influence the response of the postnatal growth of gonads, including sexual maturation, to low dose 17β-estradiol.

2. Materials and methods

2.1. Animals

Sprague–Dawley rats (Crj:CD, IGS), and ICR mice (Crj:CD-1) were purchased from Charles River, Laboratories, Inc. (Atsugi, Japan). Twenty-seven male rats (9 weeks of age), 84 female rats (8 weeks of age), 130 male mice (9 weeks of age), and 130 female mice (8 weeks of age), were used. The rats and mice arrived with mean weights of 301.1 ± 7.9 g for males and 216.2 ± 8.1 g for females, and 37.2 ± 1.2 g for males and 29.1 ± 0.9 g for females (mean ± S.D.), respectively. The animals were acclimated to the laboratory for 7–14 days prior to the start of the experiments to evaluate weight gain and any gross signs of disease or injury. The animals were housed individually in stainless steel, wire-mesh cages in a room with controlled temperature (22–25 °C) and humidity (50–65%), with lights on from 07:00 to 19:00 h daily. The animals were given access to food (NIH-07-PLD: phytoestrogen low diet, Oriental Yeast Co., Japan) and tap water through metal pipes (distilled water, Wako Pure Chem., Japan) ad libitum. In a few instances, the temperature and humidity were outside the standard ranges, but the magnitude and duration of these incidents were minimal and judged to be of no consequence. The contents of genistein and daidzein in the diet and wood bedding (ALPHA-dri, Shepherd Specialty Paper, USA) used in the present study were determined. Neither genistein nor daidzein were not detected in the diet or wood bedding (detection limit: 0.5 mg/100 g in each individual phytoestrogen, by HPLC).

Animal care and use conformed to published guidelines [18].

2.2. Experiment I (examination of intrauterine position effect on postnatal growth in rats)

2.2.1. Cesarean delivery and fostering

Estrous female rats at 10–11 weeks of age were cohabited overnight with a single male to obtain 66 pregnant females within 4 days. The next morning, females with sperm in their vaginal smears were regarded as pregnant, and this day was designated as day 0 of gestation. Thirty-three pregnant females were killed by CO_2 asphyxiation and cervical dislocation, and subjected to cesarean sectioning on day 21 of gestation. The fetuses were rapidly collected, and their intrauterine position was recorded, identified by tattoo, weighed, and sexed. Anogenital distance (AGD) was measured with a digital micrometer (reproductive precision of 0.01 mm, Digimatic caliper CD-15C, Mitutoyo Co., Kanagawa, Japan) under an Olympus dissecting microscope for each fetus, and the average was taken. The subject was held steady and in the same position during measurement. Measurements were made without knowledge of intrauterine position by one person. The AGD was measured from the center of the phallus to the center of the anus. The fetuses obtained by cesarean delivery were fostered to 33 dams that had just given birth naturally (one litter to each female). The original littermates remained together when cross-fostered. The litter sizes were similar for each cross-fostered dam. The day of cesarean section was considered as postnatal day (PND) 0. Pup body weights were recorded on PND 21 (day of weaning). Following weaning, and until 10 weeks of age, offspring were weighed once a week.

Neonates from 33 pregnant females were categorized as occupying six different intrauterine positions: 2M (male fetus located between two male fetuses; number of pups and litters on PND 0 = 36 and 19); 1M (male fetus that located between a male fetus and a female fetus; $n = 73$ and 27); 0M (male fetus located between two female fetuses; $n = 45$ and 24); 2F (female fetus located between two female fetuses; $n = 38$ and 18); 1F (female fetus located between a female fetus and a male fetus; $n = 83$ and 29); 0F (female fetus located between two male fetuses; $n = 41$ and 27). Fetuses adjacent to dead embryos (resorptions or macerated fetuses), and fetuses that were closest to each ovary or the cervix, were discarded from further analyses.

2.2.2. Observations of postnatal growth

2.2.2.1. Measurement of AGD and reproductive organ weights, and evaluation of sexual maturation. On PND

4, the AGD was measured for pups in each group using calipers with a reproductive precision of 0.01 mm. On PND 21, all pups were weaned and half of the pups in each group (2M = 13, 1M = 37, 0M = 11, 2F = 14, 1F = 43, 0F = 12) were subjected to necropsy, and the testes, epididymides, and prostates with seminal vesicles (fluid was not removed and all lobes were included) in males, and uteri and ovaries in females, were weighed. For the remaining male and female pups in each litter (2M = 21, 1M = 32, 0M = 30, 2F = 23, 1F = 36, 0F = 26), as criteria for sexual maturation, the day of vaginal opening for females (beginning on PND 28), and preputial separation for males (beginning on PND 35), were assessed, and each rat was weighed when these criteria were achieved.

2.2.2.2. *Postweaning tests of behavior, evaluation of estrous cycle, and histological observation of reproductive organs.* One male and one female were randomly selected from each litter in each group (number of rats examined: 2M = 18; 1M = 27; 0M = 25; 2F = 17; 1F = 27; 0F = 25), and were subjected to an open field test and wheel cage activity test to assess the emotionality and regulatory running activity, respectively. At 4 weeks of age, the rats were placed into a circular area (140 cm in diameter) surrounded by a wall (40 cm in height). The light and noise levels averaged 500 lx and 50 dB, respectively, at the center of the circular area. Rearing, grooming, defecation, and urination were counted, and ambulation was recorded automatically on a computer (Unicom, Inc., Japan), during a 3-min trial between 13:00 and 16:00 h on one day. At 7 weeks of age, the rats were placed into a wheel cage (Nippon Cage, Inc., Japan), 32 cm in diameter and 10 cm in width, as a measure of spontaneous activity. Each rat was kept within the wheel for 24 h with free access to food (NIH-07-PLD) and distilled water in the same animal room. The number of revolutions was automatically recorded with a 20-channel digital counter (Seiko Denki, Inc., Japan).

Each morning (9:00–10:00 h), from 6 to 10 weeks of age, all females in each group were subjected to vaginal lavage. The lavage fluid was applied to a glass slide, air-dried, and stained with Wright–Giemsa stain. Cytology was evaluated and the stage of the estrous cycle was determined using the method of Everett [19].

At 10 weeks of age, 3–5 males in each group were weighed, and anesthetized. Transcardial perfusions were carried out with a mixture of 0.1 M phosphate-buffered 1.25% glutaraldehyde and 2% paraformaldehyde. Following fixation, the prostate gland was sampled, rinsed three times in phosphate buffer, postfixed for 2 h at 4 °C in 2% osmium tetroxide, and dehydrated in alcohol; the prostate gland was embedded in epoxy resin. Ultrathin sections of the prostates were stained with uranyl acetate and lead citrate, and observed with an electron microscope (H-7100, Hitachi, Japan). The remaining males in each group (2M = 18, 1M = 27, 0M = 25) were weighed and subjected to necropsy, and the testes, epididymides, ventral prostate, and dorsal prostates with seminal vesicles, were weighed and fixed in 0.1 M phosphate-buffered 10% formalin solution. All females (2F = 17, 1F = 27, 0F = 25) were weighed and subjected to necropsy when the stage of the estrous cycle was diestrus. The ovaries and uteri were then weighed and fixed in 0.1 M phosphate-buffered 10% formalin solution. These reproductive organs were embedded in paraffin, and tissue sections were stained with H&E for light microscopy.

2.3. *Experiment II (examination of low-dose in utero effects of 17β-estradiol in mice)*

The objective of this experiment was to determine whether the intrauterine position of male fetuses, which is related to background levels of estradiol (elevated in males located between two female fetuses) and testosterone (elevated in males located between two male fetuses), would influence the response of the developing prostate to low dose 17β-estradiol. In addition, we examined whether the intrauterine position of male and female fetuses would affect the postnatal growth of other reproductive organs and sexual maturation.

2.3.1. *Administration, cesarean delivery and fostering*

Thirty female mice at 9 weeks of age were administered 17β-estradiol (Sigma Chem. Co., MO, USA) subcutaneously at a dose of 0.05 μg/kg per day for 7 days before mating, during a mating period of 7 days at the longest, and on day 0 through 17 of gestation. In a preliminary study, the offspring of the ICR pregnant females exposed to 17β-estradiol at 0.05 μg/kg per day on day 0 through 17 of gestation showed no changes in weight and histological morphology of reproductive organs in adulthood. However, the offspring of dams exposed to 17β-estradiol at 0.1 μg/kg per day on these gestational days showed changes in the parameters in adulthood (data not shown). In the present study, 30 control females were administered corn oil (Nacalai Tesque, Co., Tokyo). After the administration for 7 days before mating, female mice were caged with untreated males overnight and examined for a vaginal plug the next morning. The day on which a plug was found was termed day 0 of gestation. In this study, 30 female mice in the 17β-estradiol exposed group and the control group copulated and became pregnant. On day 18 of gestation, pregnant females were killed by CO_2 asphyxiation, and subjected to cesarean sectioning. The fetuses were rapidly collected, and their intrauterine position was recorded, identified by tattoo, weighed, and sexed, and then the AGD was measured. The fetuses obtained by cesarean delivery were fostered to 60 dams that had just given birth naturally (one litter to each female). The day of cesarean section was considered as PND 0. Pup body weights were recorded on PND 21 (day of weaning), and at 5, 7, and 10 weeks of age.

Neonates from 30 pregnant females exposed to corn oil and 30 pregnant females exposed to 17β-estradiol were categorized as occupying four different intrauterine positions: